AN ABSTRACT OF THE THESIS OF

Tyrone Daniel for the degree of Master of Science in Chemical Engineering presented on May 1, 1987.

Title: Nucleate Boiling in a Vertical Annular Duct

Redacted for Privacy

Abstract Approved: _____

Dr James G. Knudsen

Nucleate boiling of water in a vertical annulus was studied. The test section was entirely of stainless steel construction and was formed by a length of stainless steel tubing with a stainless steel heater rod centered in it. Two test sections with length to diameter ratios of 18 and 33 were used.

The purpose of this study was to determine the effect of the Reynolds number upon nucleate boiling. This was accomplished by varying the power to the test section heater from 100 - 1000 W for ten different values of the Reynolds number. The Reynolds number was varied from 32650 to 83800 for a length to diameter ratio of 18 and from 10160 to 46710 for a length to diameter ratio of 33.

Log - log plots of the heat flux versus the heater wall superheat were constructed. The data which were in the nucleate boiling regime were fit to a commonly used exponential relationship. This equation relates the heat flux to the wall superheat raised to a power n. The value of n was observed to vary from 3.08 to 1.57 for a length to

diameter ratio of 18 and 4.00 to 3.09 for a length to diameter ratio of 33.

Finally, the experimental data were compared to two correlations, that of Chen and Gungor - Winterton. Both correlations were found to predict higher values for the heat flux than were experimentally obtained.

Nucleate Boiling in a Vertical Annular Duct

by

Tyrone Daniel

A THESIS

submitted to

Oregon State University

in partial fulfillment of
the requirements for the
degree of

Master of Science

Completed May 1, 1987

Commencement June 1987

Approved:

Redacted for Privacy

Professor of Chemical Engineering in charge of major

Redacted for Privacy

Head of department of Chemical Engineering

Redacted for Privacy

Dean of Graduate School

Date thesis is presented May 1, 1987

Typed by Sheri Copans for Tyrone Daniel

To Dr. Bruce McClelland
He always had faith

Acknowledgements

The author wishes to express his sincere gratitude to the following individuals:

Dr. James G. Knudsen for his guidence and patience during the course of this work.

Dr. O. Levenspiel for his helpful suggestions.

Dr. W.J. Frederick, Dr. J. Looney and Dr. M. Kanury for serving on my committee.

Dr. Richard Turton, I guess we are supposed to meet Con in Australia and set out from there.

Constantine Kambitsis, You never could hold your beer Jimmy.

Lounes Oufer for introducing me to the world of boiling heat transfer.

Mike Mcintyre for initiating me into the wonders of MacThesis.

Nick Wannenmacher without whom this entire project would have been impossible.

Jill Mulligan and Sheri Copans for their moral support and listening to my nearly constant griping.

TABLE OF CONTENTS

LIST OF FIGURES

Nucleate Boiling in a Vertical Annular Duct

Introduction

The very high heat fluxes required in liquid cooled aircraft engines and nuclear reactors is sufficient motivation to investigate the phenomena of nucleate boiling. Very sharp increases in the heat flux are obtainable for small increases in the heated surface temperature.

These large heat transfer rates are a result of the extremely complex boiling mechanism. This results from simultaneous interactions between fluid mechanics and heat transfer. Simply put, these high heat transfer rates are due to a high degree of turbulence at the heated surface due to nucleation and the latent heat of vaporization of the fluid.

The experimental work done was that of obtaining heat flux versus wall superheat data for water at atmospheric pressure at various values of the liquid phase Reynolds number. This data was then fit to a simple exponential relationship so that the effect of the Reynolds number upon this equation's exponent could be studied.

Background

The Boiling Curve

The results of investigation into boiling heat transfer are usually plotted as the heat flux (Q/A) against heater wall surface temperature or alternatively, the wall superheat, the difference between the surface and saturation temperatures. The wall superheat being defined as the difference between the wall surface temperature and the saturation temperature of the liquid at the system pressure.

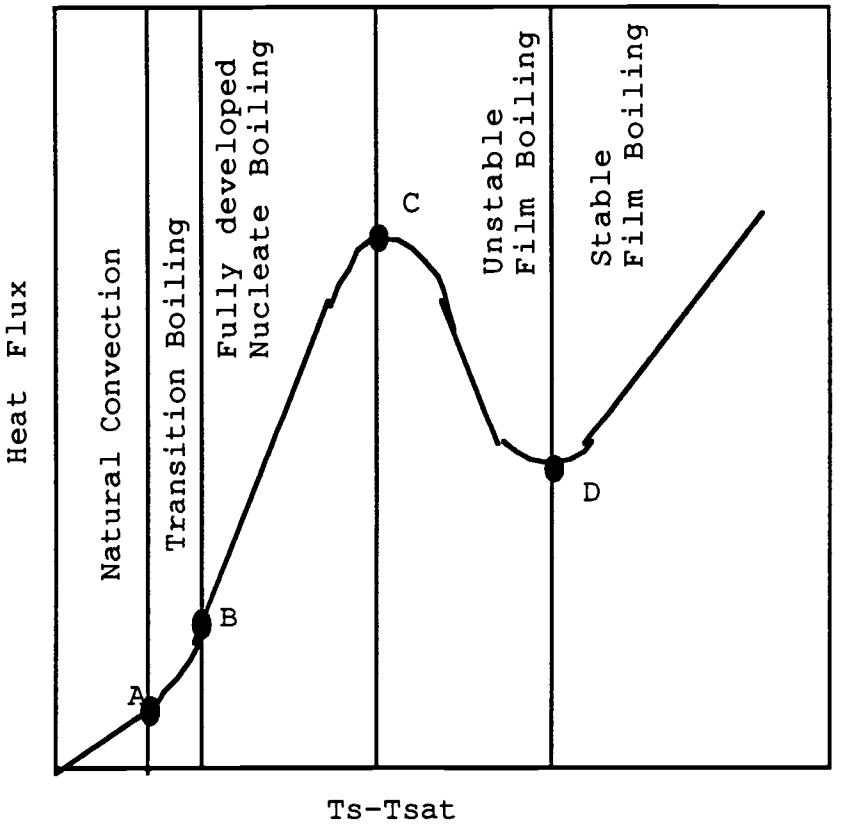

Figure 1. The boiling curve

A plot of this type is known as the "boiling curve" Figure 1 is the typical shape. Usually the curve is thought to be made up of five different heat transfer regimes. These are described as follows:

a) Convection

This is the region OA on Figure 1. The liquid may be at or below the saturation temperature. The mechanism is convective heat transfer.

b) Transition Region

The region AB on Figure 1 is known as the transition region. It is marked by the beginning of nucleation. This nucleation begins to enhance the heat transfer by disrupting the film layer next to the heater and thus the slope of the curve increases.

c) Nucleate Boiling Regime

The nucleate region is the segment BC of Figure 1. This region is characterized by fully developed boiling. Very high rates of heat transfer are attainable for very small changes in the wall superheat.

d) Critical Heat Flux

Point C on Figure 1 is known as the critical heat flux. This point marks the upper limit of the nucleate boiling region. A further increase of the heat flux at this point will cause the wall superheat to jump from C to the next stable part of the curve, E. Only under very controlled curcumstances and constant surface temperature, can the curve CDE be followed. This extreme increase in heater wall surface temperature is often to such a large degree that the heater fails. This increase in temperature is about 1000 C for water. This phenomenon is known as "burnout".

e) Unstable Film Boiling

As point C of Figure 1 is passed, an unstable vapor film forms over the heater surface. As a result of this instability, the heat transfer coefficient suddenly decreases and the heat flux is seen to decrease with increasing wall superheat.

f) Stable Film Boiling

Stable film boiling occurs as the heat flux is increased past point D. A stable film of vapor covers the entire heater surface. Vapor is released in regular intervals from the vapor film. As the heat flux is increased further radiation heat transfer becomes significant.

Flow Patterns in Boiling

Figure 2 shows a sketch of the range of flow patterns that may exist in a vertical tube with a constant heat flux applied to the wall.

The fluid enters the heated section as a subcooled liquid with a vapor quality of zero. As it moves through the tube it enters the subcooled boiling regime. In this region the wall temperature remains virtually constant, a few degrees above the saturation temperature. The bulk temperature of the fluid is increasing to saturation.

Saturated nucleate boiling is the next regime. At this point the heat transfer mechanism moves from boiling to evaporation. That is nucleation is suppressed, heat is carried away from the wall by forced convection to the surface of the liquid film, and then from the liquid surface by evaporation.

As the evaporation process reaches completion, the vapor quality reaches a value of 1 and a condition known as dryout is obtained. The mechanism of heat transfer at this point is convective heat transfer to the vapor.

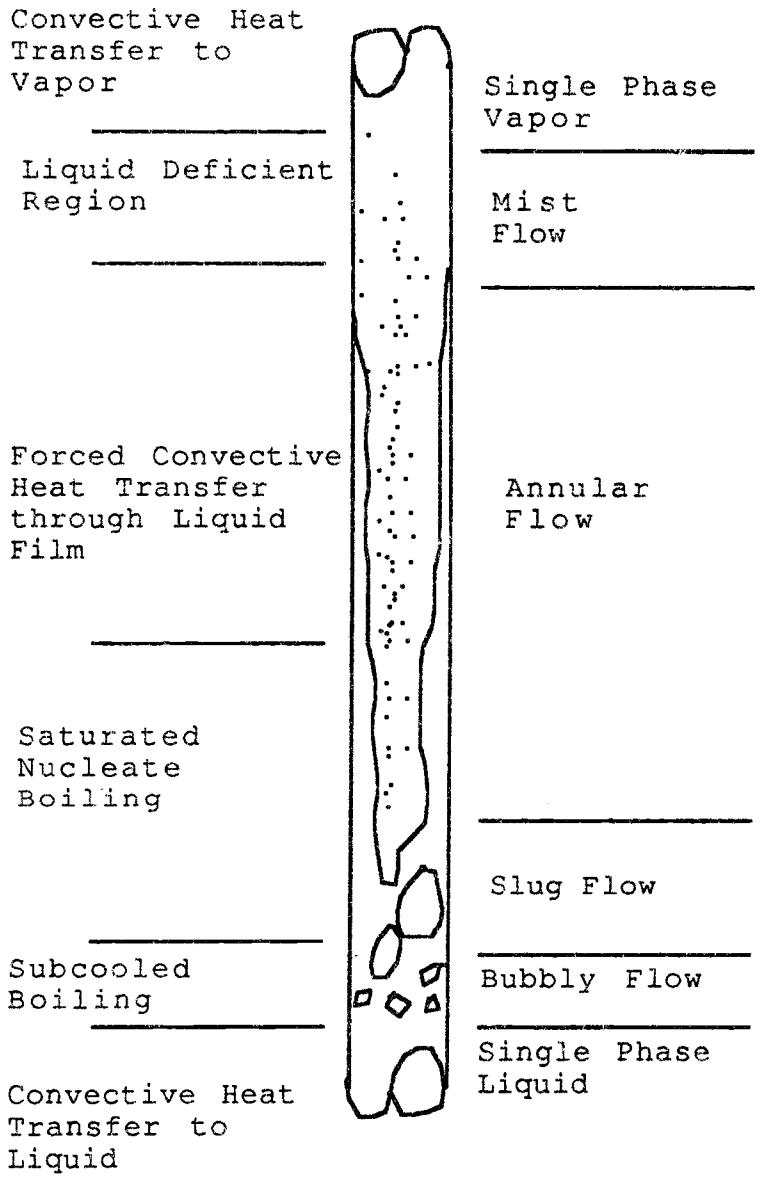

Figure 2. Flow patterns during boiling.

Vapor Formation

The formation of vapor at a heated surface occurs when the liquid temperature is increased fractionally above the corresponding saturation temperature. Vapor formation is also dependent upon the available nucleation sites.

Bubble formation in boiling fluids is postulated as follows. The mechanical equilibrium of a spherical bubble or raduis r in a liquid at constant temperature Tb and pressure P is:

$$P_s - P = \frac{2\sigma}{r} \qquad (7)$$

where,

P_s = the vapor pressure inside the bubble

σ = the surface tension of the bubble

r = the radius of the bubble

Thus a bubble will only grow if:

$$P_s > P + \frac{2\sigma}{r} \qquad (8)$$

The mechanism for bubble formation is postulated as follows. Refering to Figure 3.

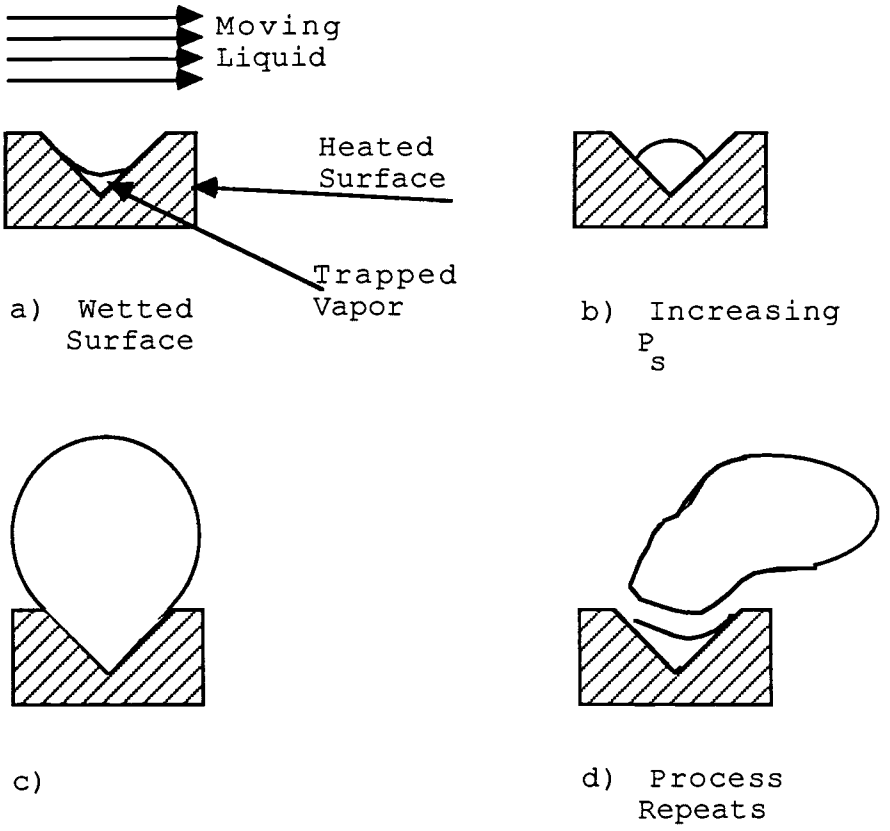

Figure 3. Bubble Formation

When the surface is first wetted, vapor is trapped within the cavities present on the surface. At this point the ambient pressure is above the vapor of the vapor.

As the heating of the surface progressed, the vapor pressure exceeds the liquid pressure thus causing the bubble to grow. Upon reaching a critical diameter the bubble is swept away leaving trapped vapor behind to repeat the process. If this postulate is accepted as true it is easy to see why surface conditions and fluid properities dramatically influence boiling.

Literature Survey

Roshenow (12), 1952 first suggested that the shape of the boiling curve could be determined by the superposition of two curves. That is, the curves for pure convection and pure pool boiling are extrapolated. These extrapolated curves are simply added together to obtain an expression for predicting the local nucleate boiling heat transfer coefficient.

The convection contribution was estimated using a Dittus - Boelter type expression:

$$h = 0.023 (Re_l)^{0.8} (Pr_l)^{0.4} \left(\frac{k_l}{de}\right) \qquad (1)$$

This equation describes the convection heat transfer coefficient as a function of the fluid velocity and the fluid properties.

The purely boiling contribution was estimated from the pool boiling correlation which was formulated by Forster and Zuber(7), 1955:

$$h_{mic} = 0.00122 \left\{ \frac{k_l^{0.79} C_{pl}^{0.45} \rho_l^{0.49} g_c^{0.25}}{\sigma^{0.5} \mu_l^{0.29} \lambda_l^{0.24} \rho_v^{0.24}} \right\} (\Delta Ts)^{0.24} (\Delta P)^{0.75} \qquad (2)$$

Chen (2) 1966, also correlated boiling heat transfer data as the summation of a pool boiling contribution and a convection contribution:

$$h = h_{mac} + h_{mic} \qquad (3)$$

The convection term being estimated by a Dittus - Boelter type equation modified by a factor, F, to account for changes in the flow due to vapor generation at high vapor qualities:

$$h = 0.023(Re_l)^{0.8}(Pr_l)^{0.4}\left(\frac{k_l}{de}\right)F \qquad (4)$$

The boiling contribution is estimated using equation (2) which is modified by a boiling suppresion factor, S to account for variations in flow.

Gungor and Winterton (9) 1985, proposed a similar correlation with the boiling heat transfer coefficient being considered to be the addition of pool boiling and convection contributions. The difference in Gungor - Wintertons correlation is the method used to calculate the pool boiling contribution. Their correlation uses an equation proposed by Cooper(6),1978:

$$hpool = 55\ \Pi r^{0.12}(-\log \Pi r)^{-0.55} M^{-0.5} Q^{0.67} S \qquad (5)$$

The suppresion factor S includes the boiling number, a dimensionless quantity as well as the Reynolds number to account for vapor generation.

An alternative method for describing the boiling curve has been proposed by many authors. The fully developed nucleate boiling regime is fitted to the simple exponential equation:

$$Q/A = C\Delta Ts^{n} \qquad (6)$$

Several researchers have suggested values for the exponent n. Thom (17),1965 suggested that the exponent n is equal to two and that the constant C is a function of the ambient pressure. Furthermore, Rohsenow (15),1985 indicates that the value of n ranges from a value of 1 for nonboiling heat transfer to upwards of 2 or 3 for fully developed nucleate boiling.

Finally, McAdams (12),1945 suggests that the value of n is constant at 3.86 and is independent of the fluid flow rate, although in this study the Reynolds number did not exceed a value of 2500.

Equipment

The equipment used in this boiling experiment was designed for the primary purpose of studying the fouling characteristics of organic fluids at high temperatures and pressures. All wetted surfaces were constructed of 316 stainless steel. A schematic diagram is shown in Figure 4. The major parts of the equipment are described below.

Test Section

The test section consists of a vertical annulus formed by a heater rod inside a 0.775 in. inside diameter , 10.75 in long tube. Heaters of two different diameters, 0.5 in. and 0.375 in. were used giving length to diameter ratios of 18 and 33 resectively. These heater rods had surface areas of 8.64 and 3.53 sq.in.. A diagram of the test section is shown in Figure 5.

Temperatures were measured by chromel-constantan thermocouples. The inside wall temperature was measured by one thermocouple buried inside the heater rod. The bulk temperatures were measured by thermocouples placed at the entrance and exit of the test section. All temperatures were measured using a Visipak digital thermometer connected to a ten position selector switch.

Power to the heater rod was controlled by a variable transformer. Power to the test section was measured by a 0-2000 Watt analog wattmeter.

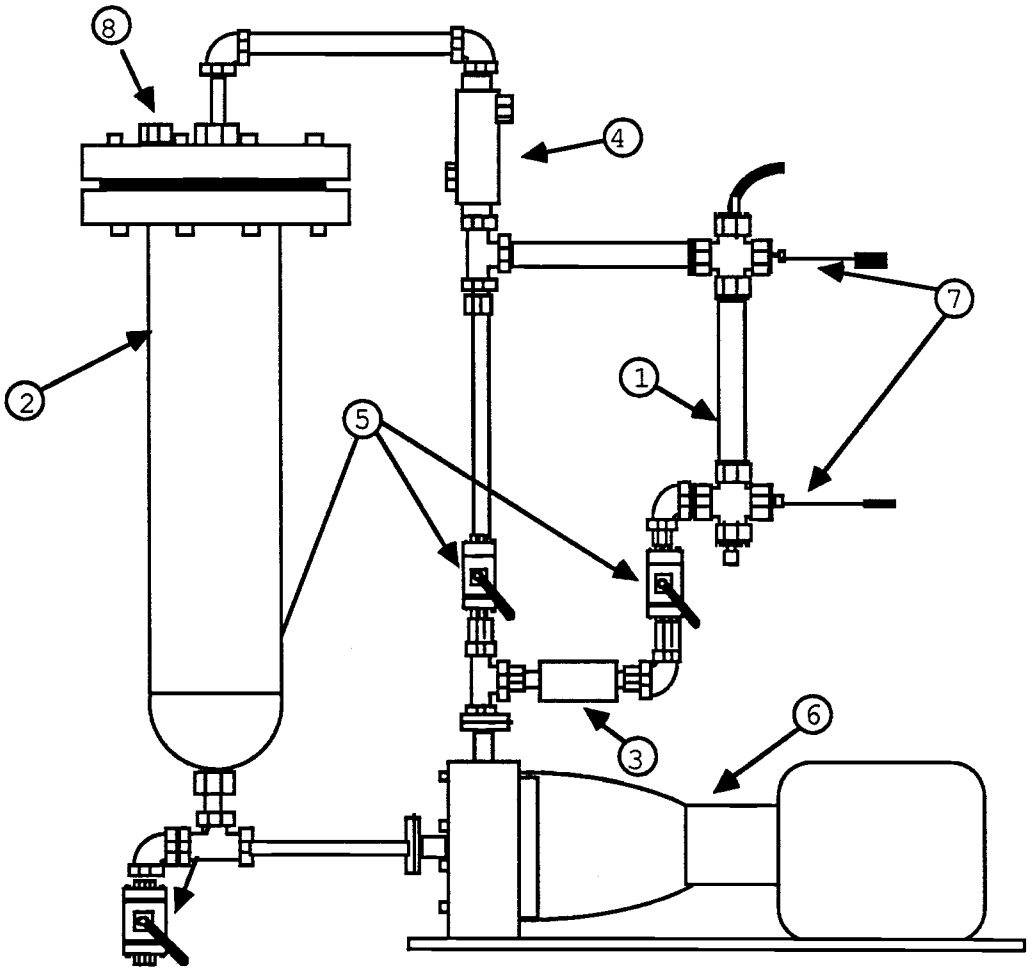

Figure 4. System Flow Diagram.

where,

1. Test Section
2. Storage Tank
3. Venturi Flow Meter
4. Cooler
5. Valves
6. Pump
7. Bulk Temperature Thermocouples
8. Fill Port

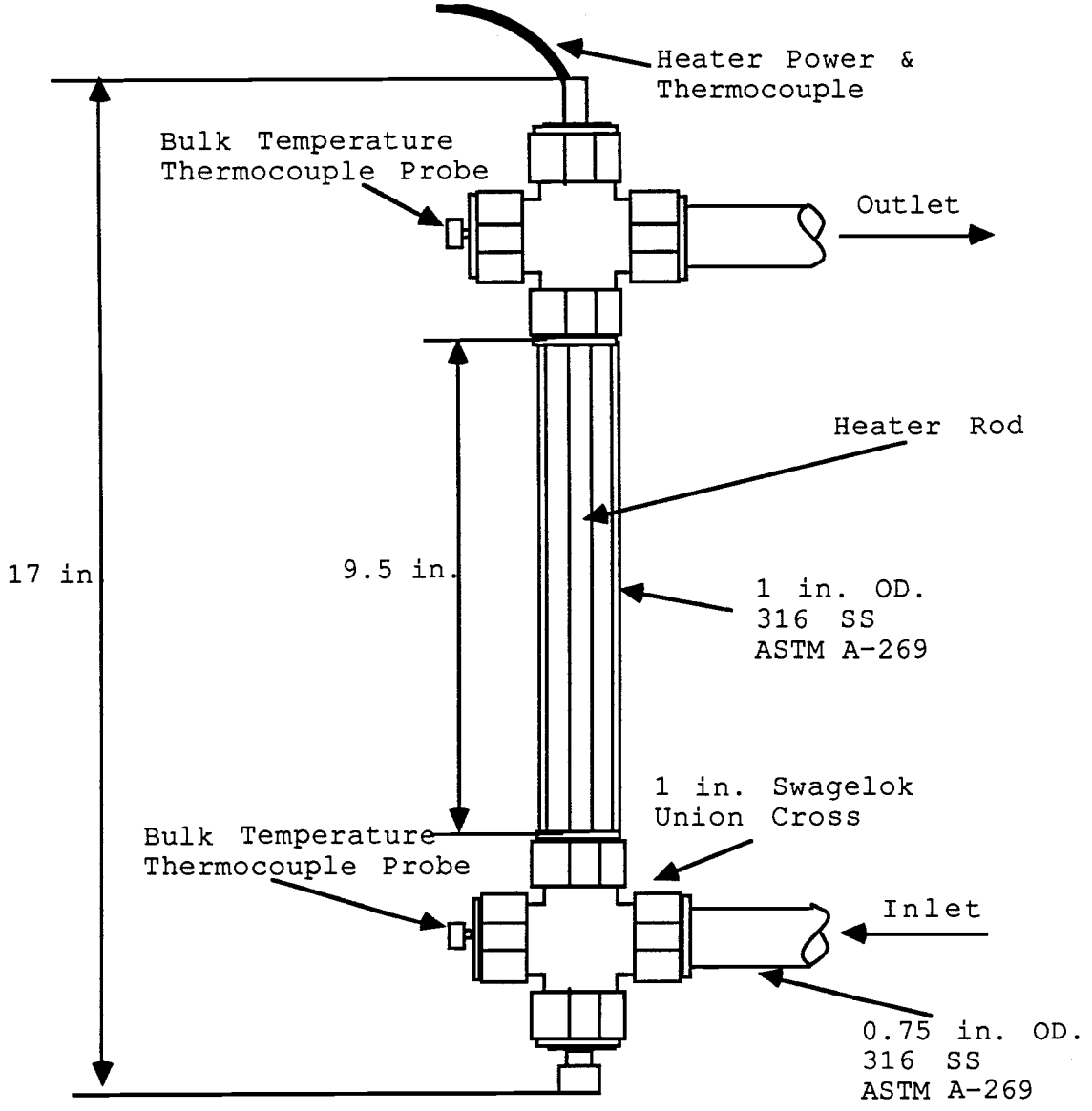

Figure 5. Test Section

Pump

Pumping requirements were met by a Kontro model HSPOH-105 stainless steel, magnetic drive sealless pump. It will produce 78 feet total differential head at 20 GPM and 3600 RPM.

This pump was selected due to it's ability to endure the 500 F, 500 psia pumping requirements of the future organic fouling studies.

Storage Tank

The storage tank was constructed of 316 stainless steel, 6 in. schedule 80 tubing 27 in. in length. The bottom of the tank was made by welding a stainless steel weld cap. The outlet of the tank consisted of 0.75 in. tubing. The top of the tank was made up of a 1500 lb. open flange welded to the schedule 80 tubing. To this flange a 1500 lb. blind flange was bolted with two penetrations in it. These were a 1 in. liquid return port and a 0.75 in. fill port. Design of the tank in this manner allows for periodic cleaning to be accomplished.

Flow Meter

Flow measurement was accomplished using a standard short nozzle venturi. The venturi was constructed of 316 stainless steel with an entrance length of five diameters and an exit length of three diameters.

The venturi was designed to produce a differential

pressure of 150 inches of water at a flow rate of ten gallons per minute. This differential pressure was measured using a Bournes model 5020 DP differential pressure cell which relates pressure difference to an output voltage. This output voltage was measured by a Fluke model 5040 digital multimeter. The calibration of the flow meter and differential cell are described in Appendix 1.

Cooler

A cooler was constructed for the apparatus to aid in maintaining the desired steady stable bulk temperature. It was constructed as a single pass, double pipe heat exchanger. A diagram of the cooler is shown in Figure 6.

A 8.5 in.length of 1.25 in. steel pipe was used for the shell side of the cooler inside of which 1 in. 316 stainless steel tubing was placed concentrically and held in place by mild steel Swagelok weld fittings welded to the steel pipe. Cooling water flows in and out through 0.5 in. Swagelok fittings.

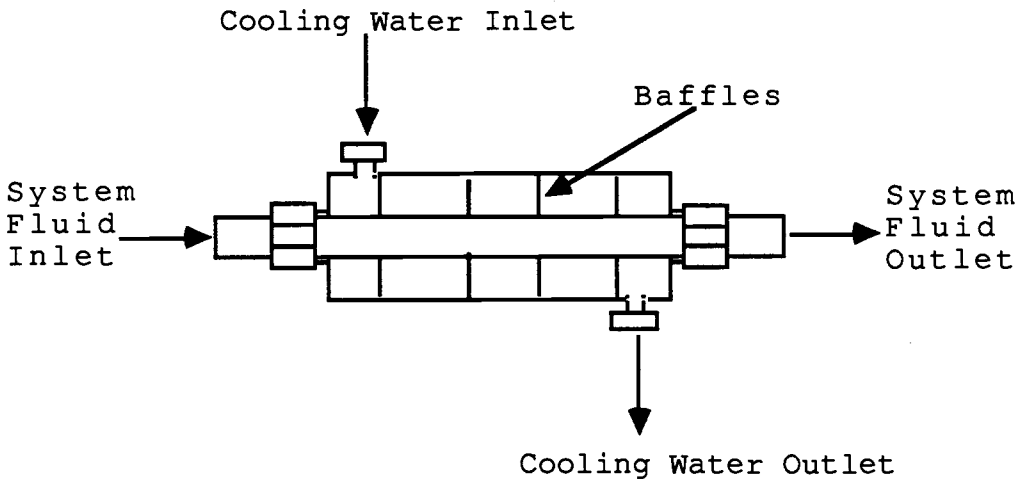

Figure 6. Cooler construction

Tubing

All tubing used in construction was either 1 or 0.75 in., 0.065 in. wall tubing. The test section used 1 in. 0.125 in. wall tubing and a 0.75 in.,0.125 in.wall modified at the ends to fit into 1 in. tubing fittings. All tubing connections were made using 316 stainless steel Swagelok tubing fittings.

Pressure Test

A pressure test was conducted in order to determine the equipments ability to withstand a 500 Psig working environment and to detect leaks in the apparatus. Since 316 stainless

steel maintains 66% of its nominal burst pressure at 500 degrees F a pressure of:

$$P = (1.66)(500) = 830 \text{ psig} \qquad (9)$$

was necessary to simulate 500 psig at 500 degrees F. Also a safety factor of 1/2 was included. Therefore the pressure test was conducted at:

$$P = (1.66)(500)(1.5) = 1245 \text{ psig} \qquad (10)$$

The equipment was filled completely with water (4.25 gal.) and a high pressure nitrogen bottle connected to the equipment. The system was pressurized to 1250 psiq and the valve to the nitrogen bottle was closed. The system was allowed to sit for one hour and no measurable decrease in pressure was observed.

Experimental Procedure

Before each run, the apparatus was rinsed with water to insure that the system was free of contaminants. This cleaning water was circulated through the system for about 15 minutes. The pump was then shut off and the system completely drained.

When this cleaning procedure was finished the apparatus was filled with 14 liters of distilled water through the fill port at the top of the tank. The system was then restarted and power to the heater rod was set at between 500 and 1000 Watts. Once the system reached the desired bulk temperature the coolant flow rate was adjusted until the desired steady stale bulk temperature was obtained. During this warm up time the differential pressure cell lines were bled through the available ports to remove any trapped air from filling the device.

Upon reaching the desired steady stable bulk temperature, the required flow rate through the test section was obtained by adjusting the test section and bypass valves simultaneously. This flow rate was maintained constant as the test proceeded. At this point, the heater power input was set at 100 W and then increased to 1000 W in increments of 100 W.

Each time the power was increased, conditions were allowed to become steady. Then the wall and bulk temperatures were recorded. The flow rate was also checked and recorded.

After 1000 W of power input was reached the power was decreased in increments of 100 W until the power input was at the 100 watt level. This was done in order to determine the reproducibility of the data. The test wall temperatures were

reproducible to within two degrees fahrenheit. At the end of each experiment the power to the heater rod was set to zero and the system drained after it had cooled to below 100 F.

Calculation Procedure

Calculation of Temperature

The surface temperature of the heated surface can be calculated from a temperature measured within the heater rod. This is accomplished by a calibration procedure proposed by Knudsen (9),1980. A temperature profile across the heater wall is shown in Figure 7.

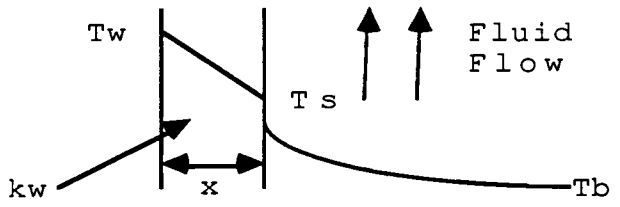

Figure 7. Temperature profile inside heater wall

Where,

Tw = the buried thermocouple temperature.

Ts the required heater surface temperature

Tb = the ambient bulk temperature of the flowing fluid.

x = the heater wall thickness.

kw = the thermal conductivity of the wall.

The overall heat transfer coefficient U is defined as the ratio of the heat flux to the total thermal driving force Tw - Tb.

$$U = \frac{Q/A}{Tw-Tb} = \frac{Q/A}{\Delta T} \qquad (11)$$

where, $\Delta T = Tw - Tb$

U is assumed to be the summation of two thermal resistances, the heater wall resistance and the convective heat transfer coefficient h:

$$\frac{1}{U} = \frac{1}{h} + \frac{x}{kw} \qquad (12)$$

The convective heat transfer coefficient, h is defined in the usual fashion:

$$h = (Q/A)/(Ts - Tb) \qquad (13)$$

The value of kw/x is determined by calibration with a known fluid (water) using Wilson's method. With the value of kw/x known the convective heat transfer coefficient, h may be determined.

$$h = \left(\frac{\Delta T}{Q/A} - \frac{x}{kw}\right)^{-1} \qquad (14)$$

The surface temperature of the heater may now be calculated by combining equations 11,12,13 and 14:

$$Ts = Tw - (Q/A)\left(\frac{x}{kw}\right) \qquad (15)$$

and for a given heat flux and wall temperature the degree of wall superheat may be calculated.

Two different heaters were used in this study. For the boiling runs with a length to diameter ratio of 18 the value of kw/x was 4023 (Btu/Hr*ft*F) and for the length to diameter ratio of 33, kw/x was 1830 (Btu/Hr*ft^2*F).

A sample calculation of wall superheat is shown in Appendix 3 .

Uncertainty Analysis

The uncertainty in the measurement of temperture was determined using the method of propagation of errors as proposed by Young (17),1975. This method assumes that a quantity N depends upon the observed quantities a,b,c.... The error E(N) which results from the errors in observation E(a),E(b),E(c)... can be represented as:

$$E(Q)=\frac{\partial Q}{\partial a}E(a)+\frac{\partial Q}{\partial b}E(b)+\frac{\partial Q}{\partial c}E(c)+..... \qquad (16)$$

The error in the measurement of Ts is thus:

$$E(Ts)=\frac{\partial Ts}{\partial Tw}E(Tw)+\frac{\partial Ts}{\partial Q}E(Q)+\frac{\partial Ts}{\partial A}E(A)+\frac{\partial Ts}{\partial (x/kw)}E(x/kw) \qquad (17)$$

Differentiating:

$$\frac{\partial Ts}{\partial Tw}=1 \qquad (18)$$

$$\frac{\partial Ts}{\partial Q}=-\frac{1}{A}\left(\frac{x}{kw}\right) \qquad (19)$$

$$\frac{\partial Ts}{\partial A}=\frac{Q}{A^2}\left(\frac{x}{kw}\right) \qquad (20)$$

$$\frac{\partial Ts}{\partial (x/kw)}=-\frac{Q}{A} \qquad (21)$$

The errors in measurement are as follows:

$E(Tw) = 2$ F from reproducibility of experinmental data

$E(Q) = 30$ Btu/Hr from wattmeter calibration

$E(A) = 0.0014\ ft^2$ from heater specifications

$E\left(\frac{x}{k_w}\right) = 0.25 \times 10^{-4}$ $Hr * ft^2 * F/Btu$ from heater calibration

Using these values, the average experimental error for all the data was found to be +6%. A sample calculation of the unexperimental uncertainty is shown in Appendix 4.

Mathmatical Modeling of Data

The data are plotted in Figures 15 to 24 in Appendix 5 in which the heat flux Q/A, is plotted versus the wall superheat, Ts - Tsat.

It is seen that the data covers three regimes of heat transfer, convection, transition to boiling and finally nucleate boiling. Since the data of interest lies in the nucleate boiling regime, only the last four or five data points were considered when the data were fitted to equation (2) except for the data from Run #4 in which no clear distinction between natural convection and nucleate boiling is

observed. The data from this run were not included in the analysis of data.

The resulting values of C and n for each boiling run were determined using least squares linear regression of the data in the nucleate boiling regime. The resulting values of C and n for each run as well as the coefficient of determination, R2 and the number of data points used to form the regression are shown in Figure's 8 and 9.

Re	n	C	R2	# POINTS
32655	3.08	1.10	0.97	4
51214	2.47	112.93	0.99	4
66175	1.61	320.60	0.96	4
83798	1.57	449.16	0.96	4
*****	****	*****	****	0

Figure 8. Results of Linear Regression for the case of L/de = 18

Re	n	C	R2	# POINTS
10158	4.00	0.0029	0.99	5
18728	4.00	0.0029	0.99	5
27444	3.20	0.0976	0.98	4
36391	2.62	1.4396	0.98	5
46714	3.09	0.2223	0.95	4

Figure 9. Results of Linear Regression for the case of L/de = 33

Chen's Correlation

Rohsenow (14),1952 first suggested that the heat transfer associated with convection and boiling can be added directly. Chen's (2),1966 correlation results from the same postulate that boiling heat transfer to saturated fluids is the summation of the ordinary macroconvection mechanism and the nucleate boiling microconvection. The individual components in Chen's correlation are modified to account for vapor generation.

The natural convective or macroconvective contribution is expressed with a Dittus - Boelter type equation:

$$h_{mac} = 0.023(Re_l)^{0.8}(Pr_l)^{0.4}\left(\frac{k_l}{de}\right)F \qquad (22)$$

where F is a correction factor based upon the ratio of the two phase Reynolds number to the liquid phase Reynolds number. This factor F is assumed to be a function of the reciprocal Martinelli parameter, 1/Xtt. This parameter is defined as:

$$1/Xtt = \left(\frac{x}{1-x}\right)^{0.9}\left(\frac{\rho_l}{\rho_v}\right)^{0.5}\left(\frac{\mu_v}{\mu_l}\right)^{0.1} \qquad (23)$$

The microconvective contribution used by Chen is the Forster and Zuber formulation for heat transfer in convection pool boiling modified by a suppresion factor S, which is a ratio of the effective superheat to the total superheat of the wall, therefore:

$$h_{mic} = 0.00122 \left\{ \frac{k_l^{0.79} C_{pl}^{0.45} \rho_l^{0.49} g_c^{0.25}}{\sigma^{0.5} \mu_l^{0.29} \lambda_l^{0.24} \rho_v^{0.24}} \right\} (\Delta Ts)^{0.24} (\Delta P)^{0.75} S \qquad (24)$$

The suppresion factor S, approaches one at zero flow rate and zero at infinite flow rate.

Finally the heat transfer coefficient is the sum of the two terms:

$$h = h_{mac} + h_{mic} \qquad (25)$$

Chen originally presented the factors F and S graphically as functions of the inverse of the Martinelli parameter 1/Xtt and the two phase Reynolds number, Re_{TP}. In the present work the

approximations proposed by Collier (6),1981 in the evaluation of F and S are used:

$$F = 1.0 \text{ for } 1/Xtt \leq 0.1 \tag{26}$$

$$F = 2.35(1/Xtt + 0.2131)^{0.736} \tag{27}$$

and

$$S = (1 + 3.31x10^{\quad}) \text{ for Re } < 32.5x10^{4} \tag{28}$$

$$S = (1 + 3.31x10^{\quad}) \text{ for } 32.5x10^{4} > \text{Re} > 70.0x10^{4} \tag{29}$$

$$S = 0.1 \text{ for Re } > 70.0x10^{4} \tag{30}$$

where,

$$1/Xtt = \left(\frac{x}{1-x}\right)^{0.9}\left(\frac{\rho_l}{\rho_v}\right)^{0.5}\left(\frac{\mu_v}{\mu_l}\right)^{0.1} \tag{23}$$

$$Re_l = \frac{(1-x)\,\rho\, u\, de}{\mu} \tag{24}$$

$$Re_{TP} = Re_l\,(F)^{1.25} \tag{25}$$

The procedure for using Chen's correlation is as follows:

a) Calculate mass flow rate:

$$m = u\rho_l Acs \qquad (26)$$

where,

$$Acs = \frac{\pi (Do^2 - Di^2)}{4} \qquad (27)$$

b) Calculate the vapor quality from an energy balance:

$$x = \frac{Q}{m\lambda} - \frac{C_{pl}(Ts - Tb)}{\lambda} \qquad (28)$$

since $Ts \approx Tb$

$$x = \frac{Q}{m\lambda} \qquad (29)$$

c) Calculate the liquid Reynolds number:

$$Re_l = \frac{(1-x)\,\rho\, u\, de}{\mu} \qquad (30)$$

d) Calculate the inverse of the Martinelli parameter with equation (23).

e) Deduce the value of the Reynolds number coefficient F

using equation 26 or 27 equation as needed.

f) Calculate the Prandtl number by:

$$Pr_l = \frac{C_{pl}\mu_l}{k_l} \qquad (31)$$

g) Calculate h_{mac} using equation 21 with de given by:

$$de = \frac{4Acs}{Pw} \qquad (32)$$

where,

Pw = wetted perimeter = π(Do +Di)

h) Calculate the two phase Reynolds number as given by equation (25)

i) Deduce the suppression factor S by either equation 27, 28 or 29 as necessary

j) Calculate h_{mic} by equation 23

k) Evaluate the total heat transfer coefficient by summing h_{mac} and h_{mic}

l) Determine the heat flux by:

$$Q/A = h\Delta Ts \qquad (33)$$

The deviation of a single data point is calculated as:

$$\text{Deviation \%} = \frac{\text{Predicted Flux - Experimental Flux}}{\text{Experimental Flux}}(100) \qquad (34)$$

The mean deviation of a data set is defined as:

$$\text{Mean Deviation \%} = \frac{\text{Sum of Absolute Deviations}}{\text{Number of Data Points}}(100) \qquad (35)$$

A sample calculation is shown in Appendix 6.

Gungor and Winterton's Correlation

Gungor and Winterton's boiling correlation was developed in order to predict flow boiling heat transfer for saturated and subcooled conditions. The equation is of the same basic form as that developed by Chen. That is, it consists of an equation which assumes boiling heat transfer is the summation of the macroconvection and microconvection contributions. To account for vapor generation Gungor and Winterton developed the coefficients E and S. These coefficients are analagous to Chen's F and S.

The convective contribution is calculated using a Dittus - Boelter equation modified by the coefficient E.

$$h_l = 0.023(Re_l)^{0.8}(Pr_l)^{0.4}\left(\frac{k_l}{de}\right)E \qquad (36)$$

where,

$$E = 1 + 24000Bo^{1.16} + 1.37(1/Xtt)^{0.86} \qquad (37)$$

$$Bo = \frac{Q}{\lambda G} \qquad (38)$$

$$1/Xtt = \left(\frac{x}{1-x}\right)^{0.9} \left(\frac{\rho_l}{\rho_v}\right)^{0.5} \left(\frac{\mu_v}{\mu_l}\right)^{0.1} \qquad (23)$$

The microconvective contribution is estimated using a correlation proposed by Cooper (6),1978:

$$h_{pool} = 55\Pi r^{0.12}(-\log\Pi r)^{-0.55} M^{-0.5} Q^{0.67} S \qquad (39)$$

where,

Πr = reduced pressure

M = molecular weight

Q = heat flux

$$S = \frac{1}{1 + 1.15x10^{-6}\ E^2\ Re_l^{1.17}} \qquad (40)$$

$$Re_l = \frac{(1-x)\ \rho\ u\ de}{\mu} \qquad (30)$$

Cooper's correlation assumes that the roughness of the tube is 1 μm. The steps for the evaluation of Gungor - Winterton's correlation are as follows:

a) Evaluate m,x,Rel and 1/Xtt using steps a) - d) on pages 29-30:

b) Calculate the boiling number:

$$Bo = \frac{Q}{\lambda G} \qquad (38)$$

c) Calculate E:

$$E = 1 + 24000Bo^{1.16} + 1.37(1/Xtt)^{0.86} \qquad (37)$$

d) Calculate h_1 using:

$$h_1 = 0.023(Re_1)^{0.8}(Pr_1)^{0.4}(\frac{k_1}{de})E \qquad (36)$$

where,

$$de = \frac{4 \text{ x flow area}}{\text{wetted perimeter}} \qquad \text{for gap} > 4 \text{ mm}$$

$$de = \frac{4 \text{ x flow area}}{\text{heated perimeter}} \qquad \text{for gap} < 4 \text{ mm}$$

e) Calculate S:

$$S = \frac{1}{1 + 1.15x10^{-6} E^2 Re_1^{1.17}} \qquad (40)$$

f) Calculate h_{pool}:

$$h_{pool} = 55\Pi r^{0.12}(-\log\Pi r)^{-0.55}M^{-0.5}Q^{0.67}S \qquad (39)$$

g) Evaluate h_{TP} as:

$$h_{TP} = h_l + h_{pool} \qquad (41)$$

h) Determine the heat flux by:

$$Q/A = h\Delta Ts \qquad (33)$$

The deviation of a data point is calculated as:

$$\text{Deviation \%} = \frac{\text{Predicted Flux - Experimental Flux}}{\text{Experimental Flux}}(100) \qquad (34)$$

The mean deviation of a data set is defined as:

$$\text{Mean Deviation \%} = \frac{\text{Sum of Absolute Deviations}}{\text{Number of Data Points}}(100) \qquad (35)$$

A sample calculation is shown in Appendix 7.

Results and Discussion

Figures 15 through 26 in Appendix 5 show plots of the heat flux, Q/A as a function of the wall superheat Ts - Tsat, each at constant flow rate and constant bulk temperature. Figure 10 shows a plot of the combined boiling data. The shape of the curves are typical and demonstrate forced convection (without boiling), transition to boiling and finally nucleate boiling. The steep portion of the curves at the right end the boiling regime and the subject of the analysis of the data.

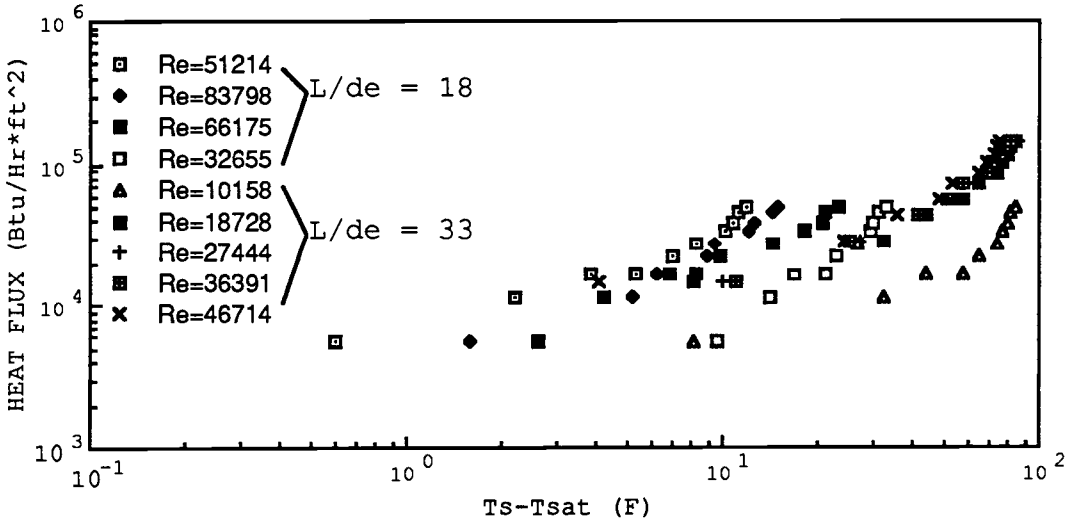

Figure 10. Combined boiling data

The slope of the line through this steep portion of the data is the exponent n in the equation:

$$Q/A = C\Delta Ts^{n} \qquad (6)$$

The value of n along the curve varies from 1 for pure convection to 3 - 4 for high heat fluxes or fully developed nucleate boiling.

As shown in Figures 8 and 9 the values of n range from 1.61 to 3.08 for a length to diameter ratio of 18 and 2.6 to 4.0 for a length to diameter ratio of 33. Examination of this Figures indicates that the exponent n is related to the inverse of the Reynolds number. That is as the Reynolds number is decreased, the value of n increases. This can also be seen graphically with Figures 11 and 12.

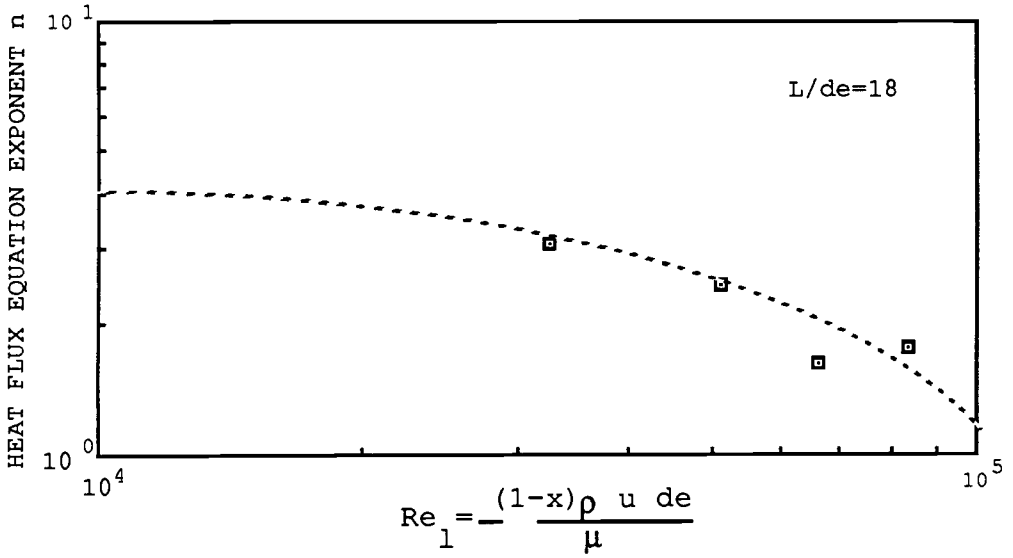

Figure 11. n versus Re for L/de of 18

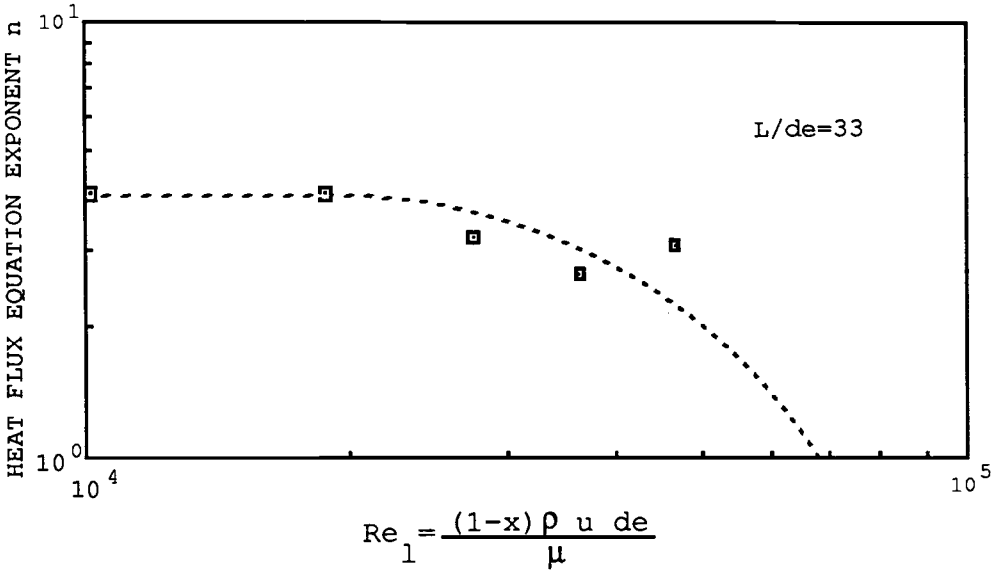

Figure 12. n versus Re for L/de of 33

The dotted line in these Figures represents a postulated value of n for various Reynolds numbers . When the Reynolds number is equal to zero (no flow) n is equal to a limiting value of 3 - 4 in agreement with published values for nucleate pool boiling. As the Reynolds number is increased the value of n decreases, apparently to a value of 1 as pure convection is approached. This result is in good agreement with the findings of previous investigations.

An interesting point to note is that the Reynolds number may also be increased by increasing the effective diameter of

the anulus, de. This change in de is reflected in the length to diameter ratios used in this study since the actual entrance length to the test section was a constant. Therefore an increase in de will lower L/de and increase the Reynolds number for a given velocity. That is, as the equivalent diameter is increased, pool boiling becomes dominant over the convection contribution. The data presented also supports this result.

A graphical comparison of experimental data with Chen's correlation is shown in Figure 13. The experimental local heat transfer coefficient is plotted on the y - axis against the heat transfer coefficient predicted by Chen's correlation on the x - axis. Examination of these plots shows that most of the plotted points fall below the 45 degree line. This indicates that the correlation consislently predicts higher heat transfer coefficients than were obtained experimentally. Chen's correlation gave an average absolute deviation of 11.9% with a maximum absolute deviation of 51% and a minimum absolute of 0% for a length to diameter of 18. These are reasonable deviations for boiling data. For a length to diameter ratio of 33, Chen's correlation gave average, maximum and minimum absolute deviations of 56%, 75% and 27% respectively. The deviation in predicted and experimental values increased with the local heat transfer coefficient. Since Chen's correlations consistently predicts higher coefficient than were measured a slight modification of the equation is probably necessary. However, this should not be done until more data are obtained. Since two different heaters were used, surface conditions could have contributed to the greater deviation observed with the L/de = 33 case.

Gungor - Winterton's correlation is presented graphically in Figure 14 as a plot of experimental heat transfer

coefficient on the y - axis with Gungor - Winterton's predicted heat transfer coefficient on the x - axis. Gungor - Winterton's also predicted consistently higher values of the heat transfer coefficient although to a larger degree than Chen's correlation. This correlation gave an average absolute deviation of 202% and a minimum absolute deviation of 3.1% for a length to diameter ratio of 33. The length to diameter ratio of 18 gave average, maximum and minimum deviations of 302%, 399% and 27.5%. These deviations also increased as the heat flux increased.

Both correlations indicated a very low pure boiling contribution for a length to diameter ratio of 18. This influenced a decision to increase the available heat flux so that more of the boiling curve could be studied thus resulting in the investigation of the case for L/de = 33.

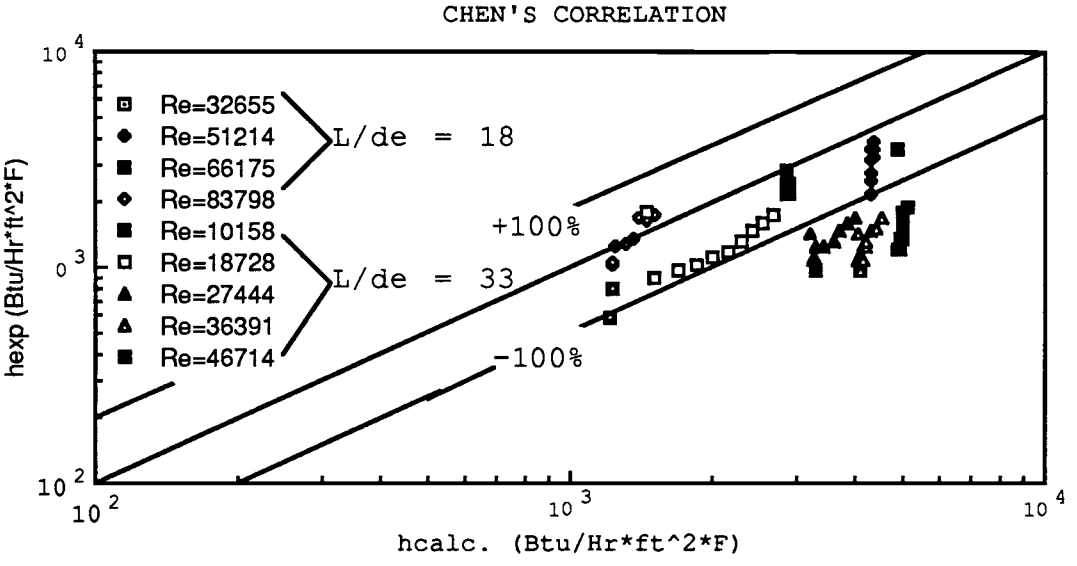

Figure 13. Chen's Correlation

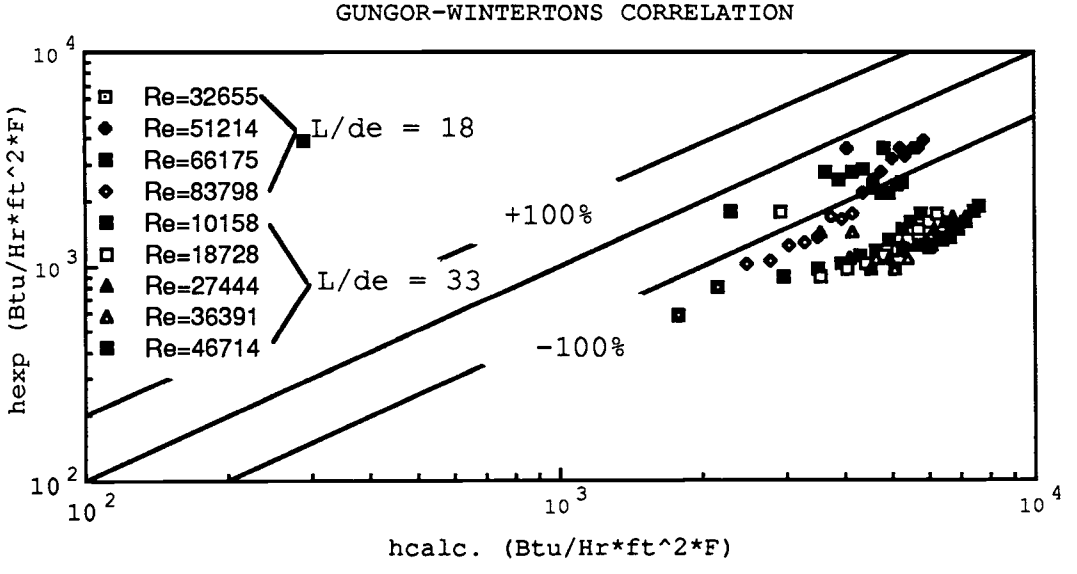

Figure 14. Gungor - Winterton's Correlation

Conclusions and Recommendations

Nucleate boiling of water flowing in an annulus was studied with the effect of Reynolds number and length to diameter ratio as the major parameters. The data were correlated to an equation of the form:

$$Q/A = \Delta Ts^n$$

The value of n was found to range from 1.57 to 3.08 for a length to diameter ratio of 18 and 2.62 to 4.00 for length to diameter ratio of 33. Thus the value of the exponent n was found to range from a value of 4.00 to approaching 1 as the Reynolds number went from 10160 to 83800. These results agree with previously reported data.

Comparison with Chen's and Gungor - Winterton's correlations was helpful in deciding to use a higher heat flux so that more data could be obtained in the fully developed mucleate boiling regime. Higher heat fluxes produced data which more fully reflected the findings of other researchers.

Both Gungor-Winterton and Chen's correlations consistently predict higher values for the heat transfer coefficient, with Chen's correlations giving better results than the Gungor - Winterton correlation. Both correlations used the same additive method for predicting the heat transfer coefficient, the only difference being the method by which the coefficients F and S for Chen's

correlation and E and S for Gungor - Winterton's correlation are calculated.

Since the magnitude of the boiling contribution was small compared to the total magnitude of the heat transfer coefficient and the convection contribution was estimated in the same manner for both correlations, it is reasonable to assume that the method used to evaluate the coefficient F and E for Chen's and Gungor - Winterton's correlations are affected by the length to diameter ratio of the annulus. That is, as the length to diameter ratio is increased, the absolute deviations for both correlations increase.

Chen's correlation is not affected by changing the length to diameter ratio to the extent that the Gungor - Winterton correlation is. This is in spite of the fact that both methods for estimating the equivalent diameter for Gungor - Winterton's correlation were used. The best results being obtained when the heated diameter was used in this correlation.

Recommendations for future work are as follows:

1) Further studies at higher heat fluxes although this increases the risk of burning out a heater.

2) Further studies at higher Reynolds numbers in an attempt to determine if the exponent n approaches 1.

3) Use greater care to insure the system is not contaminated.

4) Use more accurate instruments for measurements of temperature aand flow rate.

.

.

.

Nomenclature

A:	Heater surface area	[ft^2]
A_{cs}:	Annulus cross sectional area	[ft^2]
Bo:	Boiling number	[ ]
C:	Exponential equation constant	[ ]
C_{pl}:	Heat capacity of liquid	[Btu/Hr*lb*F]
d_e:	Annulus equivalent diameter	[ft]
Di:	Outside diameter of the heater	[ft]
Do:	Inside diameter the annulus	[ft]
g_c:	Gravitational constant	[lb*ft/lb*Hr]
G:	Mass flux through test section	[lbm/Hr*ft^2]
h:	Convective heat transfer coefficient	[Btu/Hr*ft F]
h_{mic}:	Microconvective heat transfer coefficient	[Btu/Hr*ft F]
h_{pool}:	Pool boiling heat transfer coefficient	[Btu/Hr*ft F]
k_l:	Liquid thermal conductivity	[Btu/Hr*ft*F]
k_w:	Heater wall thermal conductivity	[Btu/Hr*ft*F]
L:	Test section entrance length	[ft]
M:	Molecular weight	[ ]
m:	Mass flow rate through test section	[lbm/Hr]
n:	Heat transfer equation exponent	[ ]
P:	Ambient pressure	[lbf/ft]
Pr :	Liquid Prandtl number	[ ]
P_s:	Vapor pressure of liquid	[lbf/ft^2]
Q:	Power	[W]
Re_l :	Liquid phase Reynolds number	[ ]

Re_{TP}:	Two phase Reynolds number	[ ]
S:	Bubble suppresion factor	[ ]
Tb:	Bulk fluid temperature	[F]
Ts:	Heater surface area	[ft^2]
Tsat:	Fluid saturation temperature	[F]
U:	Overall heat transfer coefficient	[Btu/Hr*ft^2]
u:	Fluid velocity through test section	[ft/s]
Xtt:	Martinelli two phase parameter	[ ]
X :	Heater wall thickness	[ft]
x:	Vapor quality	[ ]

Greek Symbols

ΔTs:	Wall superheat	[F]
λ:	Latent heat of vaporization	[Btu/Hr*lbm]
μ_l:	Liquid phase viscosity	[lb/ft*Hr]
μ_v:	Vapor phase viscosity	[lb/ft*Hr]
Πr:	Reduced Pressure	[ ]
ρ_l:	Liquid phase density	[lb/ft^3]
ρ_v:	Vapor phase density	[lb/ft^3]

Bibliography

1) Bergles, A.E. and Rohsenow, W.M., 'The Determination of Forced Convection Surface Boiling Heat Transfer', Trans. ASME, J. Heat Transfer, Vol. 86, pp.305-311, 1964.

2) Chen, J.C., 'Correlations for Boiling Heat Transfer to Saturated Fluids in Convective Flow', I.E.C. Process Des. Dev., Vol. 5, No. 3, pp. 322-329, 1966.

3) Chernobyl'skii, I.I. and Tananaiko, I.M., 'Heat Exchange during Boiling of Liquids in Narrow Annular Tubes', Sov. Phys. Techn. Phys., pp.2244-2249, 1956.

4) Collier, J.G., Convective Boiling and Condensation, 2nd Ed., McGraw-Hill, pp. 206-247, 1972.

5) Collier, J.G., 'Forced Convective Boiling', Two-Phase Flow and Heat Transfer in the Power and Process Industries, Eds. Bergles, A.E., Collier, J.G., Delhaye, J.M., Hewitt, G.F. and Mayinger, F., Hemisphere, pp. 226-255, 1981.

6) Cooper, M.G., 'Nucleate Boiling', Proc. of the Sixth Int. Heat Transfer Conf., Vol. 6, Toronto, Canada, Aug. 1978, pp. 463-469.

7) CRC Handbook of Chemistry and Physics, 64th Ed., CRC Press, 1983.

8) Gungor, K.E. and Winterton, R.H.S., 'A General Correlation for Flow Boiling in Tubes and Annuli',International Journal of Heat and Mass Transfer., Vol 29, No.3 , pp351-358,Mar. 1986

9) Forster, H.K. and Zuber, N., AIChE J., Vol. 1, No. 4, pp. 531-535, 1955.

10) Knudsen, J.G., 'Apparatus and Techniques for Measurements of Fouling of Heat Transfer Surfaces', Condenser Boifouling Control, eds. Garey, J.F.,Jorden, R.M., Aitken, A.H., Burton, D.T. and Gray, R.H., EPRI Symp. Proc., Atlanta, Georgia, Mar. 25-29, 1979 Ann Arbor Science, pp. 143-168, 1980.

11) Knudsen, J.G. and Katz, D.L., Fluid Dynamics and Heat Transfer, McGraw-Hill, 1958.

12) McAdams, W.H., Kennel, W.E., Minden, C.S., Carl, R., Picornell, P.M. and Dew, J.E., 'Heat Transfer at High Rates to Water with Surface Boiling', Ind. Eng. Chem., Vol. 451 pp 1945-1953, 1949.

13) Perry's Chemical Engineers' Handbook, 6th. Ed., McGraw-Hill, 1984.

14) Rohsenow, W.M., 'A Method of Correlating Heat Transfer Data for Surface Boiing Liquids', Trans. ASME, Vol.74, pp. 969-975, 1952.

15) Rohsenow,W.M., Hartnett, J.P. and Ganic, E.N. Heat Transfer Fundamentals, 2nd Ed., McGraw-Hill, Chap. 12, 1985.

16) Shah, M.M., "Generalized Prediction of Heat Transfer During Subcooled Boiling in Annuli', Heat Transfer Eng., Vol. 4, No 1, pp 24-31, 1983.

17) Thom, J.R.S., Walker, W.M.,Fallen, T.A. and Reising, G. F.S., 'Boiling in Subcooled Water During Flow up Heated Tubes or Annuli', Proc. Inst. Mech. Eng., Vol. 180, Pt. 3C, pp. 226-246, 1965-1966.

18) Young, H.D., 'Statistical Treatment of Experimental Data', McGraw-Hill, 1962.

APPENDICES

Appendix 1

Experimental Data

BOILING RUN #1 Re=83798 L/de=18 u=11.65 ft/s

Q	Q/A	Tb	ΔTs
(WATTS)	(Btu/Hr*ft^2)	(F)	(F)
100	5688.3	206.0	0.6
200	11376.6	206.0	2.2
300	17064.9	205.0	3.8
400	22753.2	205.0	5.3
500	28441.5	205.0	6.9
600	34129.8	206.0	8.3
700	39818.1	206.0	10.1
800	45506.4	206.0	10.7
900	51194.7	206.0	11.3
1000	56883.0	205.0	11.9
100	5688.3	206.0	0.6
200	11376.6	206.0	2.2
300	17064.9	205.0	3.8
400	22753.2	205.0	5.3
500	28441.5	205.0	6.9
600	34129.8	206.0	8.3
700	39818.1	206.0	10.1
800	45506.4	206.0	10.7
900	51194.7	206.0	11.3
1000	56883.0	205.0	11.9

BOILING RUN #2 Re=66175 L/de=18 u=9.20 ft/s

Q	Q/A	Tb	ΔTs
(WATTS)	(Btu/Hr*ft^2)	(F)	(F)
100	5688.3	205.0	1.6
200	11376.6	205.0	5.2
300	17064.9	205.0	6.2
400	22753.2	205.0	8.3
500	28441.5	205.0	8.9
600	34129.8	206.0	9.5
700	39818.1	206.0	12.1
800	45506.4	206.0	12.7
900	51194.7	206.0	14.3
1000	56883.0	205.0	14.9
100	5688.3	205.0	1.6
200	11376.6	205.0	5.2
300	17064.9	206.0	6.2
400	22753.2	206.0	8.3
500	28441.5	206.0	8.9
600	34129.8	206.0	9.5
700	39818.1	206.0	12.1
800	45506.4	206.0	12.7
900	51194.7	206.0	14.3
1000	56883.0	207.0	13.9

BOILING RUN #3 Re=49379 L/de=18 u=6.87ft/s

Q	Q/A	Tb	ΔTs
(WATTS)	(Btu/Hr*ft^2)	(F)	(F)
100	5688.3	206.0	2.6
200	11376.6	206.0	4.2
300	17064.9	206.0	6.8
400	22753.2	206.0	8.3
500	28441.5	206.0	9.9
600	34129.8	205.0	14.5
700	39818.1	206.0	18.1
800	45506.4	207.0	20.7
900	51194.7	207.0	21.3
1000	56883.0	206.0	23.4
100	5688.3	206.0	2.6
200	11376.6	206.0	4.2
300	17064.9	206.0	6.8
400	22753.2	206.0	8.3
500	28441.5	206.0	9.9
600	34129.8	207.0	14.5
700	39818.1	207.0	18.1
800	45506.4	207.0	20.7
900	51194.7	207.0	21.3
1000	56883.0	207.0	23.4

BOILING RUN #4 Re=32655 L/de=18 u=4.54 ft/s

Q	Q/A	Tb	ΔTs
(WATTS)	(Btu/Hr*ft^2)	(F)	(F)
100	5688.3	205.0	4.5
200	11376.6	205.0	8.2
300	17064.9	206.0	10.8
400	22753.2	206.0	14.3
500	28441.5	206.0	15.9
600	34129.8	205.0	18.5
700	39818.1	207.0	20.1
800	45506.4	207.0	24.7
900	51194.7	207.0	25.3
1000	56883.0	206.0	25.9
100	5688.3	205.0	4.5
200	11376.6	206.0	8.2
300	17064.9	206.0	10.8
400	22753.2	206.0	14.3
500	28441.5	206.0	15.9
600	34129.8	206.0	18.5
700	39818.1	207.0	20.1
800	45506.4	206.0	24.7
900	51194.7	207.0	25.3
1000	56883.0	207.0	26.9

BOILING RUN #5 Re=16747 L/de=18 u=2.33 ft/s

Q (WATTS)	Q/A (Btu/Hr*ft^2)	Tb (F)	ΔTs (F)
100	5688.3	205.0	4.5
200	11376.6	205.0	8.2
300	17064.9	206.0	10.8
400	22753.2	206.0	14.3
500	28441.5	206.0	15.9
600	34129.8	205.0	18.5
700	39818.1	207.0	20.1
800	45506.4	207.0	24.7
900	51194.7	207.0	25.3
1000	56883.0	206.0	25.9
100	5688.3	206.0	4.5
200	11376.6	206.0	8.2
300	17064.9	206.0	10.8
400	22753.2	205.0	14.3
500	28441.5	206.0	15.9
600	34129.8	206.0	18.5
700	39818.1	206.0	20.1
800	45506.4	206.0	24.7
900	51194.7	207.0	25.3
1000	56883.0	207.0	25.9

BOILING RUN #6 Re=10158 L/de=33 u=2.5 ft/s

Q	Q/A	Tb	ΔTs
(WATTS)	(Btu/Hr*ft^2)	(F)	(F)
100	14540.4	212.0	8.1
200	29080.8	212.0	32.1
300	43621.2	212.0	44.2
400	58161.6	212.0	57.2
500	72702.0	212.0	64.3
600	87242.4	212.0	73.3
700	101782.8	212.0	76.4
800	116323.2	212.0	79.4
900	130863.6	212.0	81.5
1000	145404.0	212.0	83.5
100	14540.4	212.0	8.1
200	29080.8	212.0	33.1
300	43621.2	212.0	44.2
400	58161.6	212.0	57.2
500	72702.0	212.0	64.3
600	87242.4	212.0	72.3
700	101782.8	212.0	76.4
800	116323.2	212.0	79.4
900	130863.6	212.0	81.5
1000	145404.0	212.0	83.5

BOILING RUN #7 Re=18728 L/de=33 u=4.68 ft/s

Q	Q/A	Tb	ΔTs
(WATTS)	(Btu/Hr*ft^2)	(F)	(F)
100	14540.4	212.0	8.1
200	29080.8	212.0	32.1
300	43621.2	212.0	44.2
400	58161.6	212.0	57.2
500	72702.0	212.0	64.3
600	87242.4	212.0	73.3
700	101782.8	212.0	76.4
800	116323.2	212.0	79.4
900	130863.6	212.0	81.5
1000	145404.0	212.0	83.5
100	14540.4	212.0	10.1
200	29080.8	212.0	29.1
300	43621.2	212.0	42.2
400	58161.6	212.0	55.2
500	72702.0	212.0	63.3
600	87242.4	212.0	71.3
700	101782.8	212.0	76.4
800	116323.2	212.0	78.4
900	130863.6	212.0	81.5
1000	145404.0	212.0	83.5

BOILING RUN #8 Re=27444 L/de=33 u=6.86 ft/s

Q	Q/A	Tb	ΔTs
(WATTS)	(Btu/Hr*ft^2)	(F)	(F)
100	14540.4	212.0	10.1
200	29080.8	212.0	27.1
300	43621.2	212.0	44.2
400	58161.6	212.0	54.2
500	72702.0	212.0	58.3
600	87242.4	212.0	69.3
700	101782.8	212.0	76.4
800	116323.2	212.0	79.4
900	130863.6	212.0	81.5
1000	145404.0	212.0	85.5
100	14540.4	212.0	11.1
200	29080.8	212.0	26.1
300	43621.2	212.0	39.2
400	58161.6	212.0	51.2
500	72702.0	212.0	58.3
600	87242.4	212.0	67.3
700	101782.8	212.0	69.4
800	116323.2	212.0	75.4
900	130863.6	212.0	77.5
1000	145404.0	212.0	80.5

BOILING RUN #9 Re=36391 L/de=33 u=9.1ft/s

Q	Q/A	Tb	ΔTs
(WATTS)	(Btu/Hr*ft^2)	(F)	(F)
100	14540.4	212.0	11.1
200	29080.8	212.0	25.1
300	43621.2	212.0	41.2
400	58161.6	212.0	51.2
500	72702.0	212.0	57.3
600	87242.4	212.0	68.3
700	101782.8	212.0	71.4
800	116323.2	212.0	74.4
900	130863.6	212.0	78.5
1000	145404.0	212.0	81.5
100	14540.4	212.0	11.1
200	29080.8	212.0	26.1
300	43621.2	212.0	39.2
400	58161.6	212.0	51.2
500	72702.0	212.0	58.3
600	87242.4	212.0	67.3
700	101782.8	212.0	69.4
800	116323.2	212.0	75.4
900	130863.6	212.0	77.5
1000	145404.0	212.0	80.5

BOILING RUN #1C Re=46714 L/de=33 u=11.68 ft/s

Q (WATTS)	Q/A (Btu/Hr*ft^2)	Tb (F)	ΔTs (F)
100	14540.4	212.0	4.1
200	29080.8	212.0	24.1
300	43621.2	212.0	35.2
400	58161.6	212.0	48.2
500	72702.0	212.0	53.3
600	87242.4	212.0	64.3
700	101782.8	212.0	68.4
800	116323.2	212.0	72.4
900	130863.6	212.0	73.5
1000	145404.0	212.0	75.5
100	14540.4	212.0	5.1
200	29080.8	212.0	24.1
300	43621.2	212.0	36.2
400	58161.6	212.0	46.2
500	72702.0	212.0	54.3
600	87242.4	212.0	63.3
700	101782.8	212.0	67.4
800	116323.2	212.0	70.4
900	130863.6	212.0	72.5
1000	145404.0	212.0	76.5

Appendix 2

Calibration of the flow meter

The differential pressure cell used was a Bournes, model 5020 DP two wire differential pressure transmitter. Differential pressures are detected using a variable capacitor which converts a differential pressure input to a millivolt output. The differential pressure cell was powered by a 15 volt Analog Devices (AD 405) power supply. Voltage output during the calibration were measured using a Fluke 8050 A digital multimeter.

The following sequence of steps were followed to calibrate the differential pressure transducer:

1) The temperature of the water used during the calibration was recorded.
2) The differential pressure cell zero was set. (0.300 V for 0.0 differential pressure).
3) The span was set to give 1.00 A for 10 GPM.
4) The span and zero were checked and reset if necessary.
5) The differential pressure input versus voltage output were recorded for a range of zero to 150 inches of water.

After the differential pressure cell was

calibrated, the results were checked. Thje calibration curve for the transduce was found to be within 4.13% of the actual values for differential pressures above five inches of water.

Appendix 3

Sample Calculation of Surface Temperature

Given: L/de = 33, Tw = 231.5, x/k_w = 1/1830

Q/A = 116323

Ts = 231.5 - (116323)(1/1830) = 222.7 F

ΔTs = 222.7 - 212.0 = 10.7 F

Appendix 4
Sample Calculation of Experimental Uncertainty

Sample calculation of Experimental Uncertainty

Given:

L/de = 33, A = 0.0245 sq.ft., Q = 2730 Btu/Hr

Ts = 222.7 F, x/kw = 1/1830 Hr*ft^2*F/Btu

$$\frac{\partial Ts}{\partial Tw} = 1$$

$$\frac{\partial Ts}{\partial Q} = -\frac{1}{0.0245}\left(\frac{1}{1830}\right) = -2.23 \times 10^{-2}$$

$$\frac{\partial Ts}{\partial A} = \frac{2730}{(0.0245)^2}\frac{1}{1830} = 2485.3$$

$$\frac{\partial Ts}{\partial (x/kw)} = -\frac{2730}{0.0245} = -111429$$

$$E(Ts) = (1(2) + (-2.23 \times 10^{-4})(30) + (2485.3)(0.0014) + (-111429)(0.25 \times 10^{-4})$$

$$E(Ts) = 2.0 \text{ F}$$

$$E(Ts)\% = \frac{2}{222.7}(100) = 0.9\%$$

Appendix 5
Plots of heat flux versus wall superheat

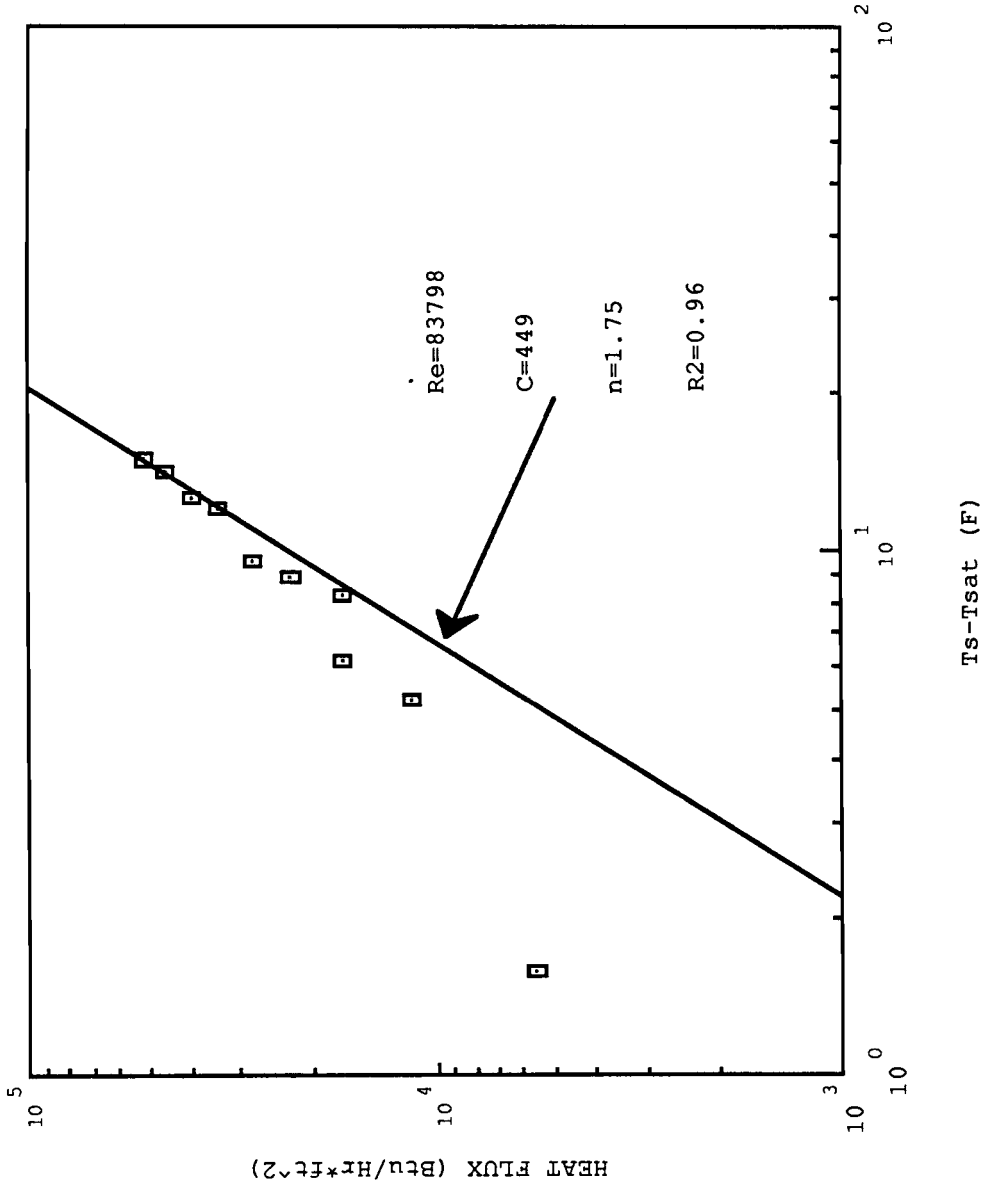

Figure 15 . Boiling Run #1

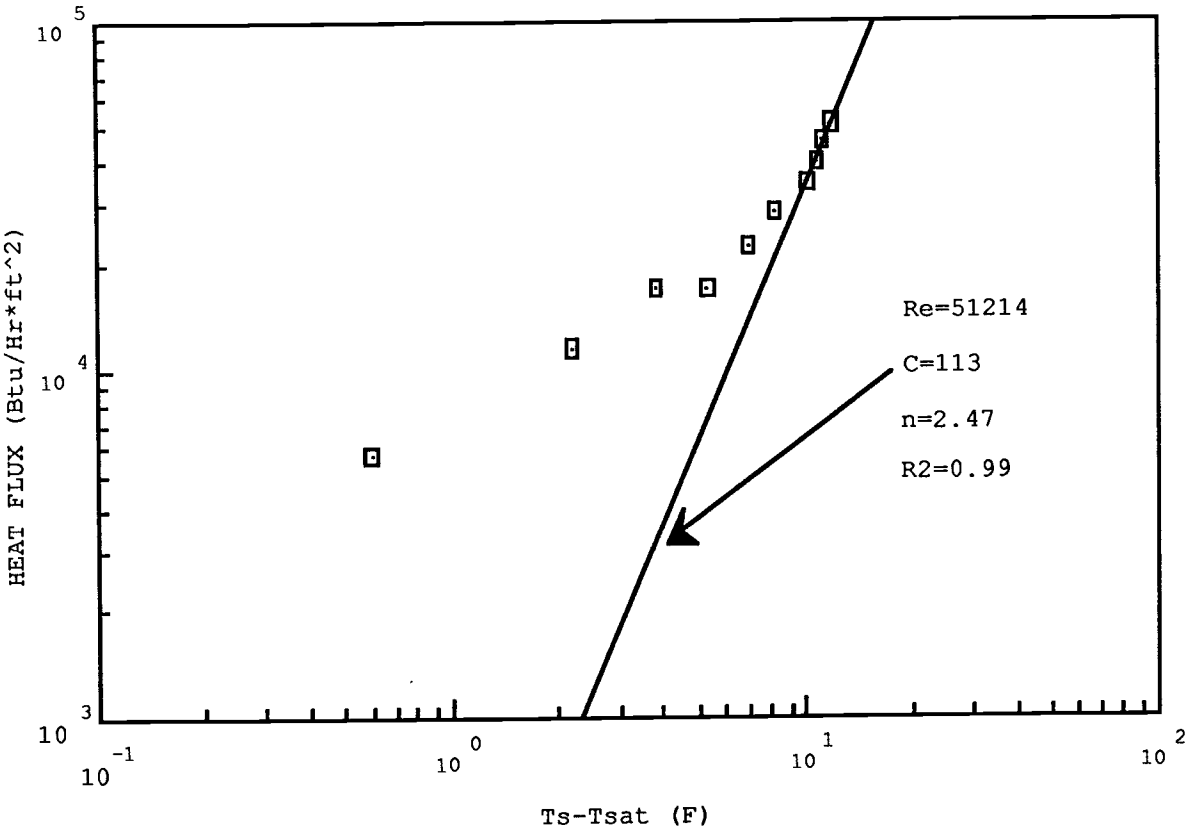

Figure 16. Boiling Run #2

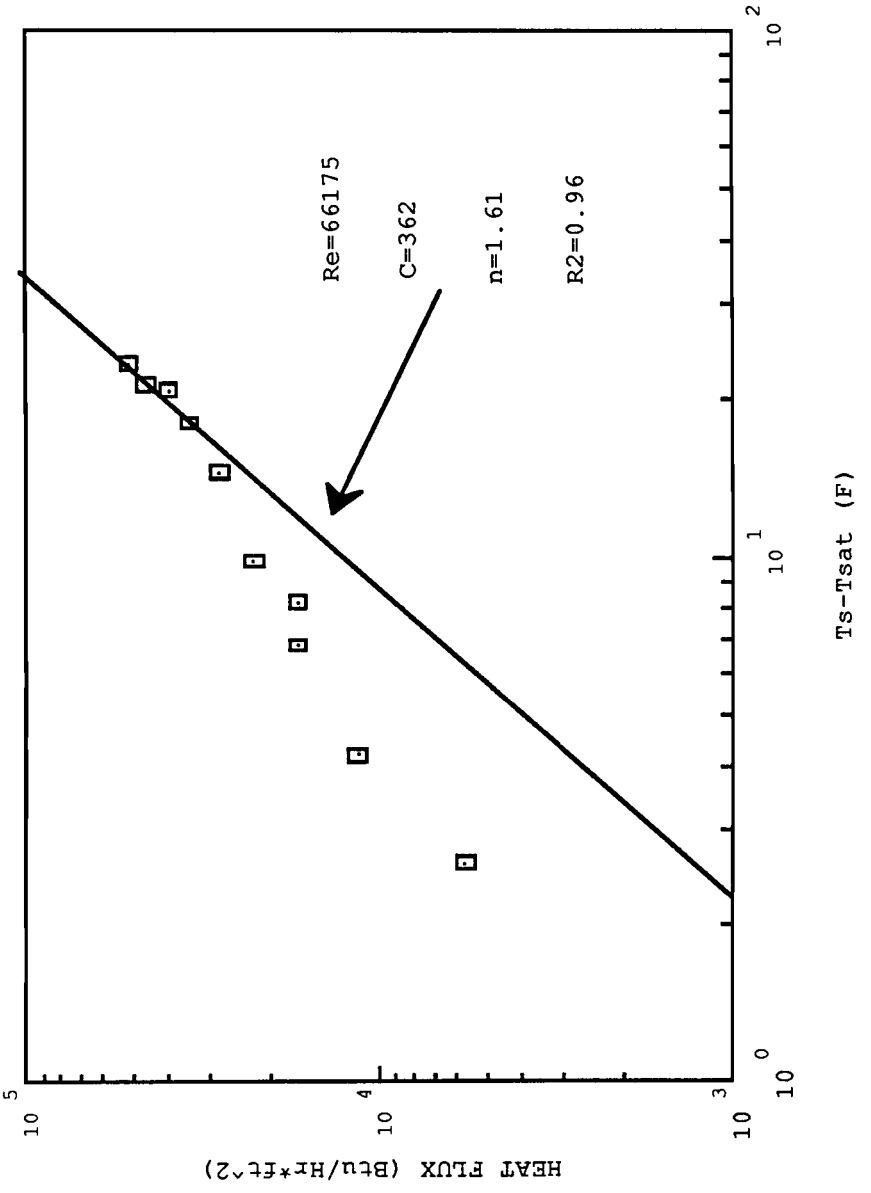

Figure 17. Boiling Run #3

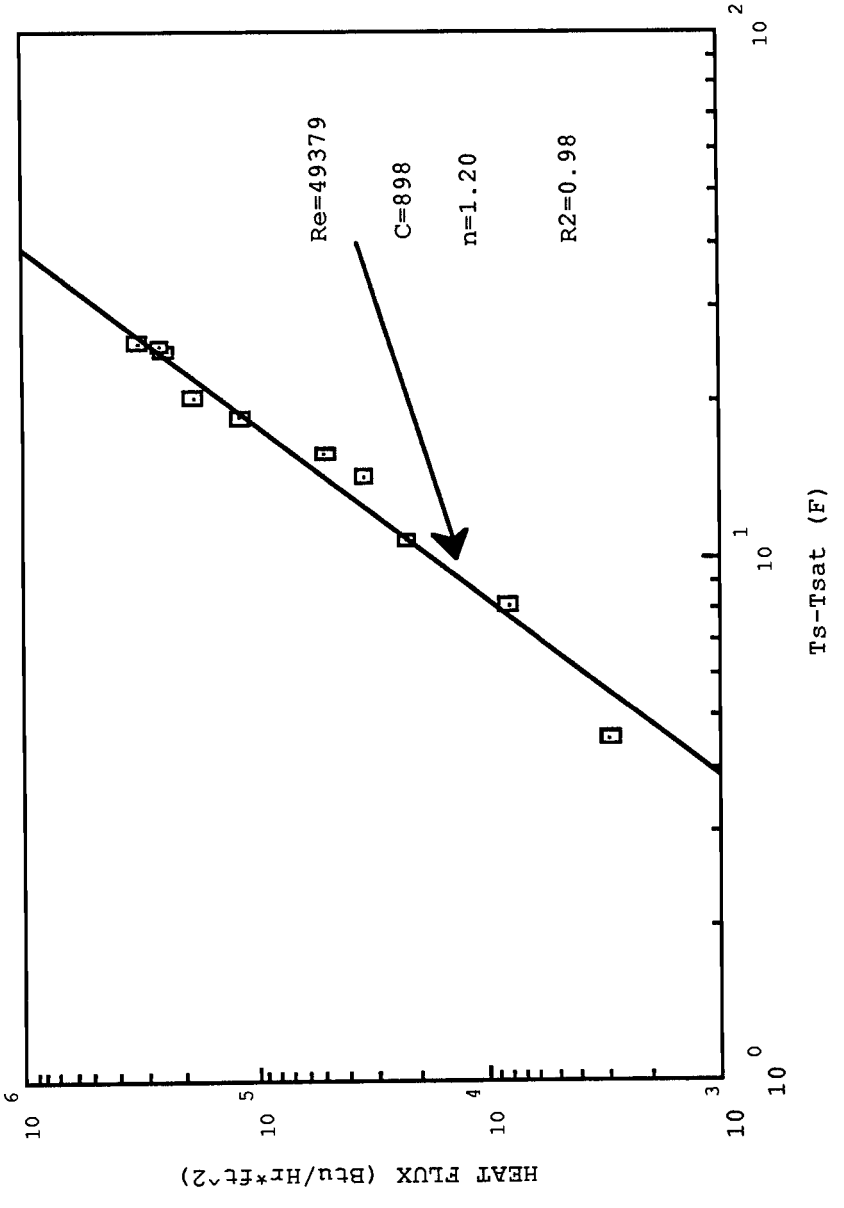

Figure 18. Boiling Run #4

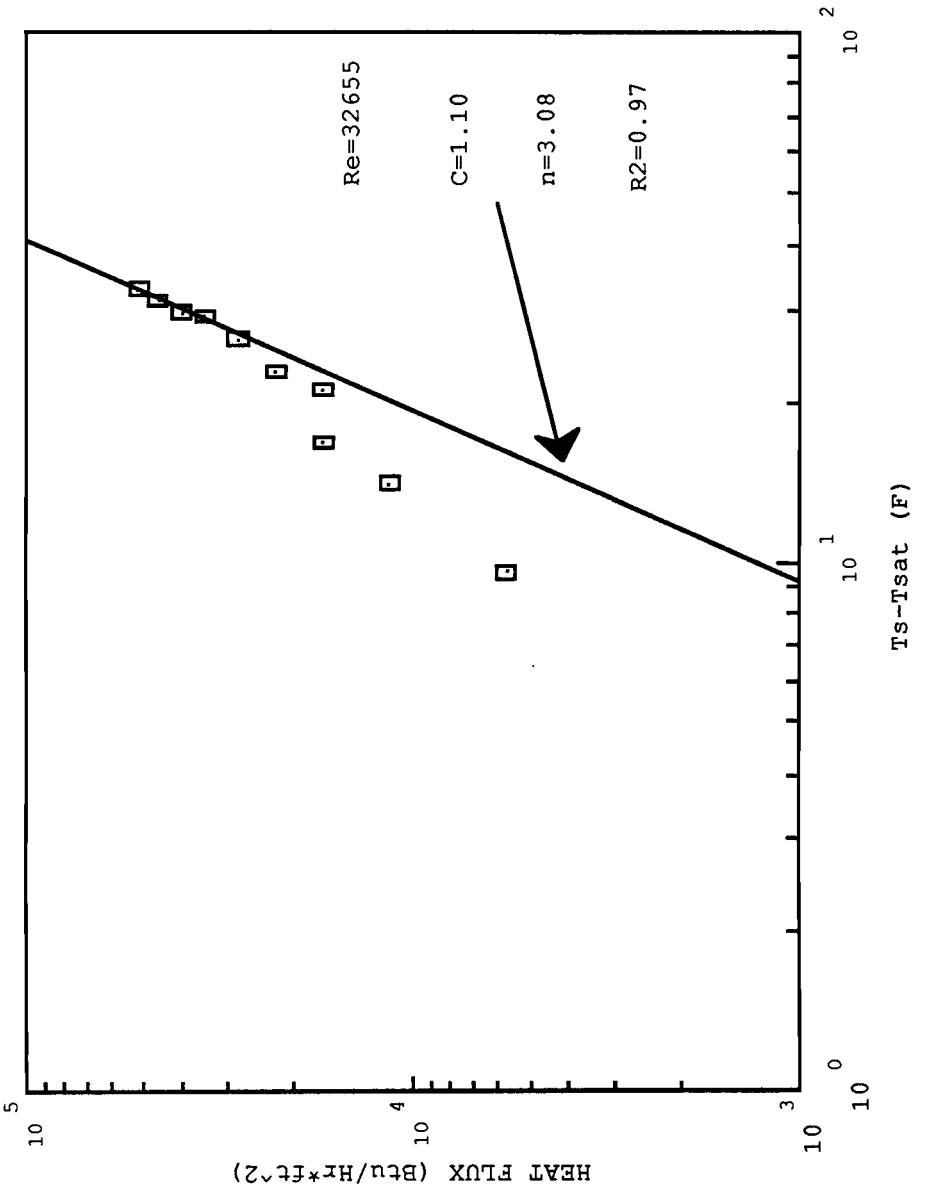

Figure 19. Boiling Run #5

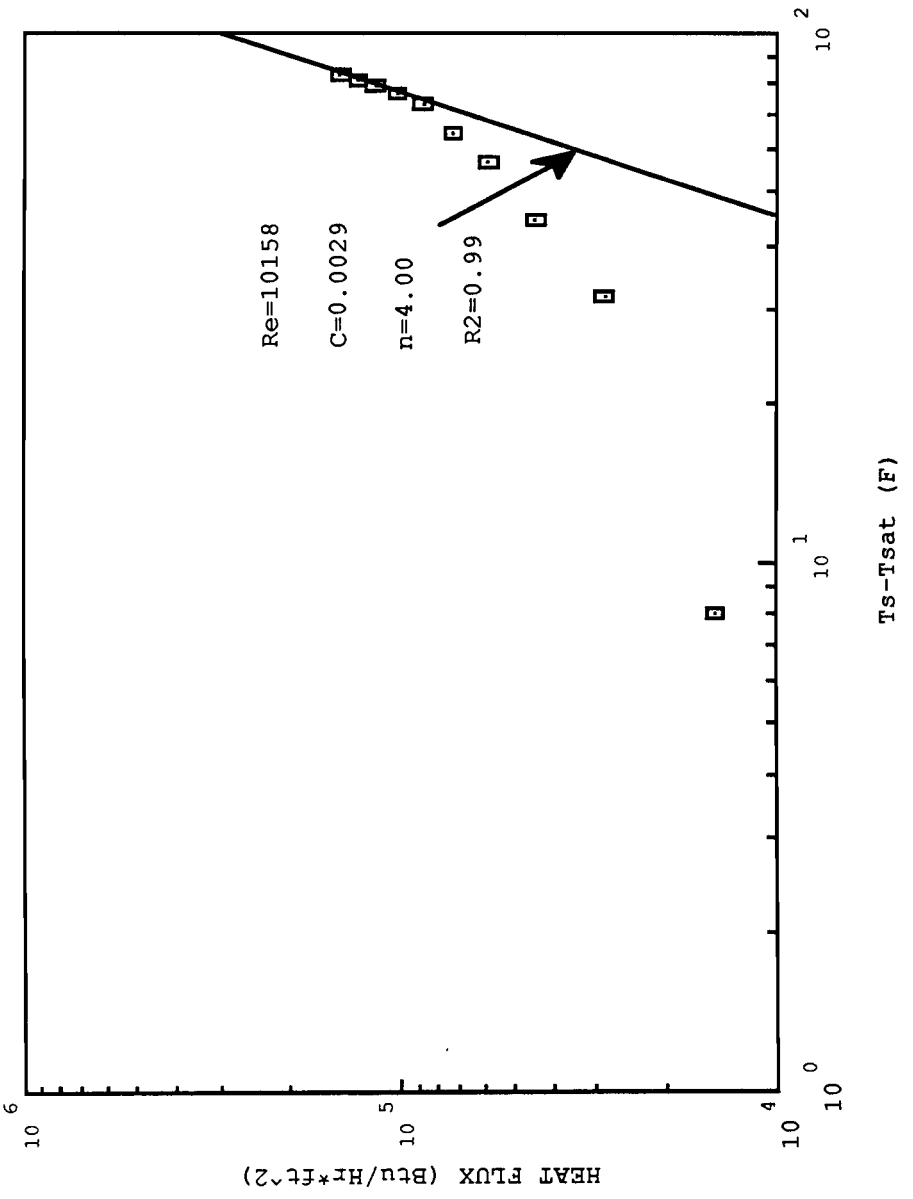

Figure 20. Boiling Run #6

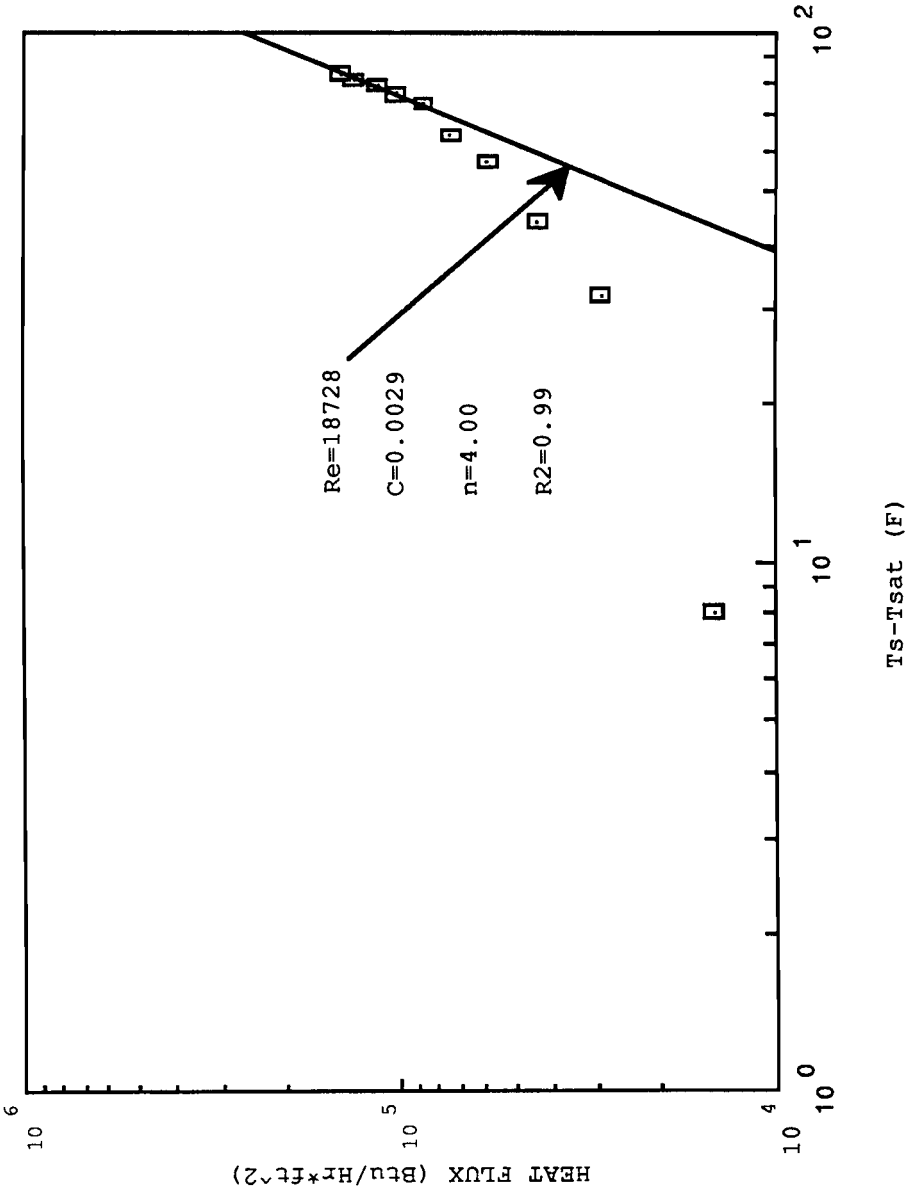

Figure 21.Boiling Run #7

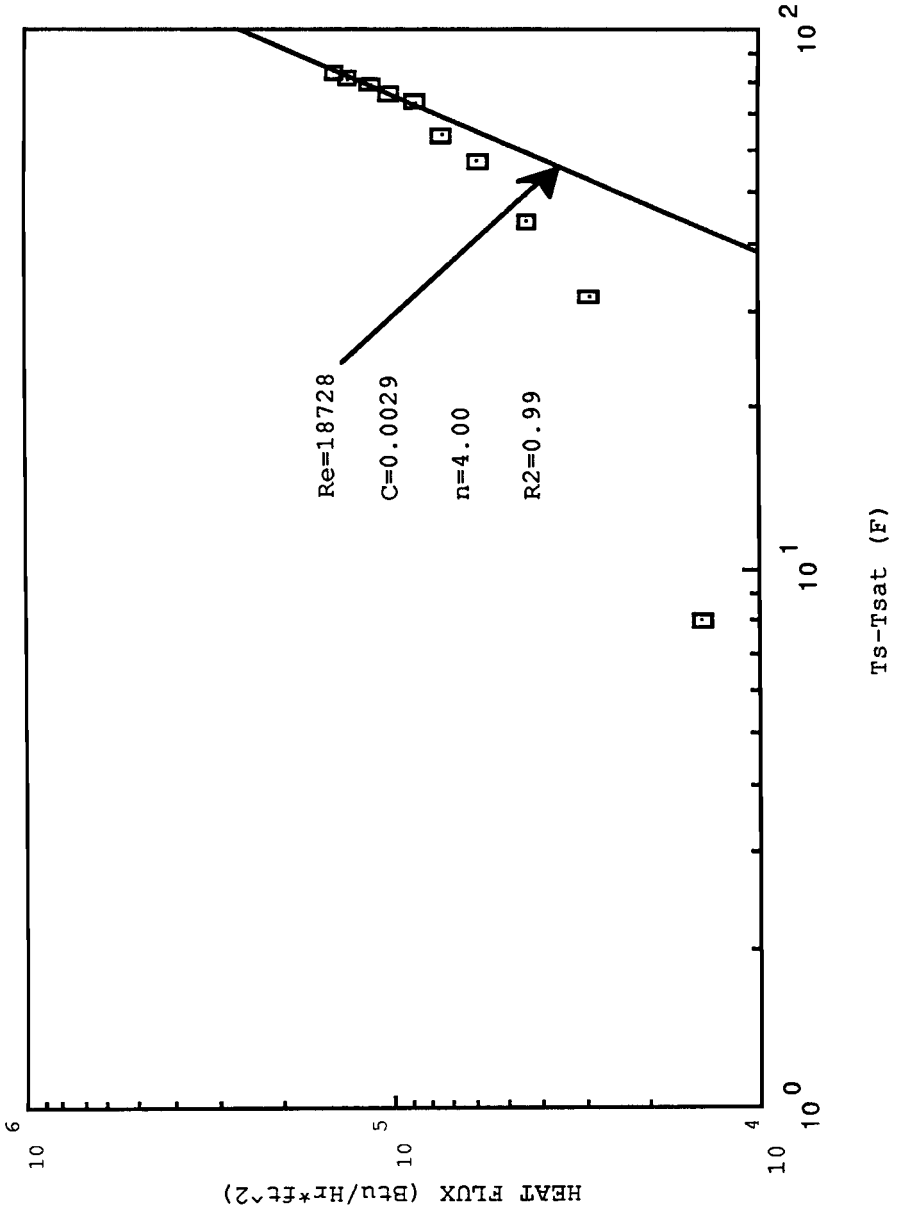

Figure 22. Boiling Run #8

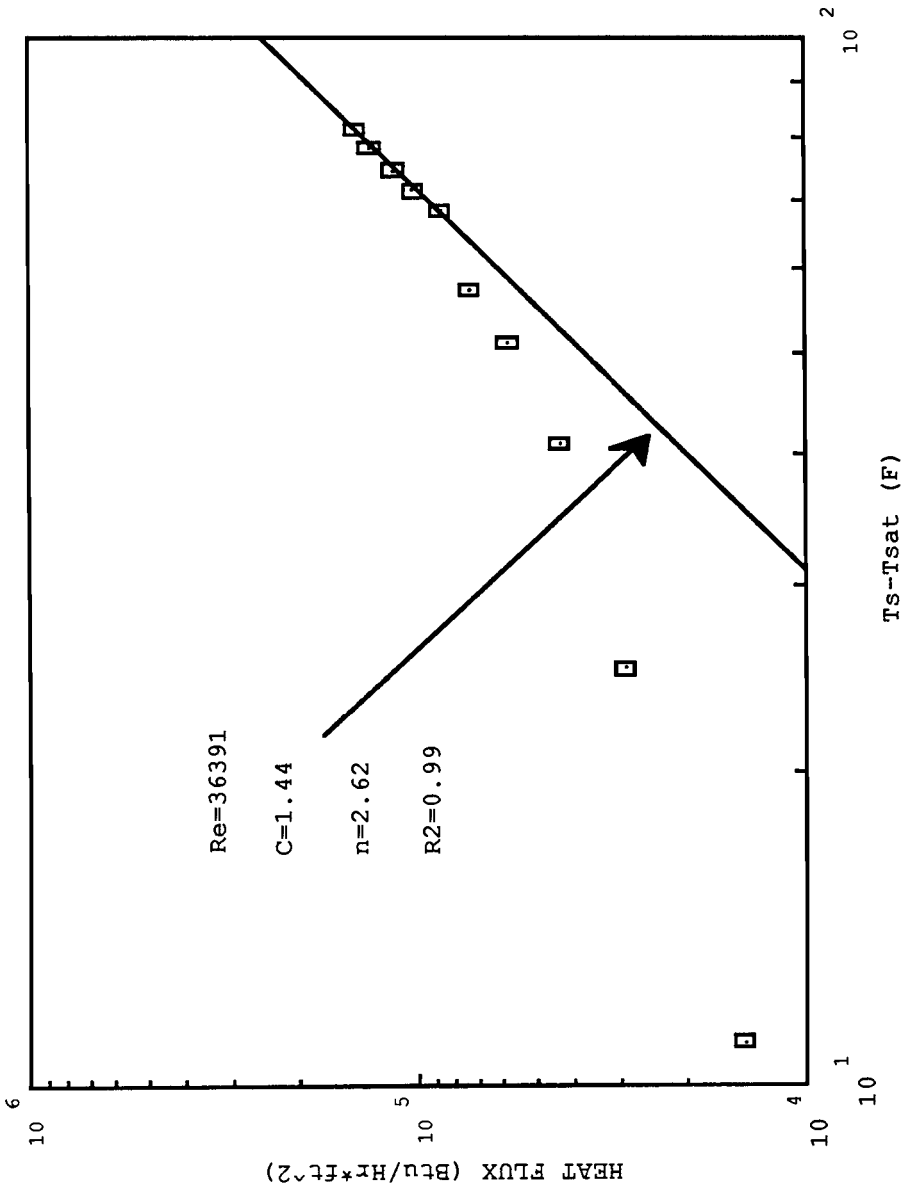

Figure 23. Boiling Run #9

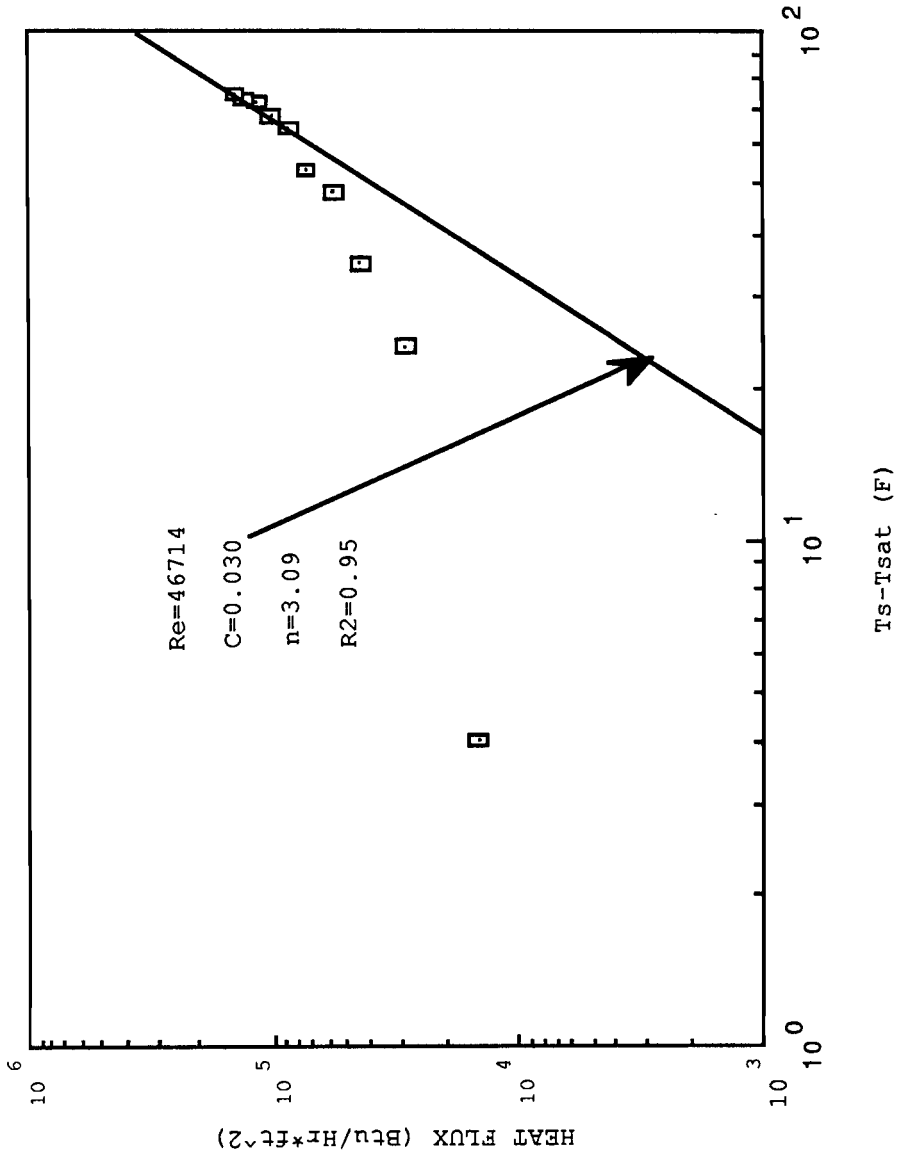

Figure 24. Boiling Run #10

Appendix 6 and 7: Correlations

Appendix 6
Sample calculation of heat flux predicted by Chen's correlation

Given:

L/de = 33, de = 0.0125 ft, Acs = 7.36x10

Q = 800 W = 2730 Btu/Hr, ΔTs = 72.4 F

u = 11.68 ft/s = 42048 ft/Hr

Using the calculation procedure on page

a) $m = (42048)(59.8)(7.36\times10^{-4}) = 1851$

b) $x = \frac{2730}{(1851)(972.9)} = 0.002$

c) $Re_l = \frac{(1 - 0.002)(0.0125)(1851)}{(0.673)(7.36\times10^{-4})} = 46714$

d) $1/Xtt = \left(\frac{0.002}{1-0.002}\right)^{0.9}\left(\frac{59.8}{0.0367}\right)^{0.5}\left(\frac{0.03}{0.673}\right)^{0.1} = 0.11$

e) $F = 2.35(0.11 + 0.213)^{0.736}$

f) $Pr = \frac{(1.0076)(0.673)}{(0.394)} = 1.72$

g) $hmac = 0.023(46714)^{0.8}(1.72)^{0.4}\left(\frac{0.394}{0.0125}\right)(1.02) = 4997$

h) $Re_{TP} = (46714)(1.02) = 47885$

i) S = (1 + 3.31x10 (47885)) = 0.86

$$h)\ hmic = \left\{(0.00122)\ \frac{(0.394)^{0.79}(1.0076)^{0.45}(59.8)^{0.49}(4.17\times10^{8})^{0.25}}{(41.83\times10^{-4})^{0.5}(0.673)^{0.29}(972.9)^{0.24}(0.0367)^{0.24}}\right\}$$

$$\times\ \left\{(72.4)^{0.24}(40.5)^{0.75}(0.86)\right\} = 177$$

k) $h = 4997 + 177 = 5175$

i) $(Q/A)_{pred} = 5175(72.4) = 374670$

j) $\text{Deviation\%} = \frac{374670 - 116323}{374670}(100) = 68.9\%$

Appendix 7

Sample calculation of heat flux predicted by Gungor - Winterton's correlation

Given:

L/de = 33, de = 0.0125 ft, Acs = 7.36×10^{-4}

Q = 800 W = 2730 Btu/Hr, ΔTs = 72.4 F

u = 11.68 ft/s = 42048 ft/Hr

Using the calculation procedure on page

a) $m = (42048)(59.8)(7.36 \times 10^{-4})$

$$x = \frac{2730}{(1851)(972.9)} = 0.002$$

$$Re_l = \frac{(1 - 0.002)(0.0125)(1851)}{(0.673)(7.36 \times 10^{-4})} = 46714$$

$$1/Xtt = \left(\frac{0.002}{1-0.002}\right)^{0.9}\left(\frac{59.8}{0.0367}\right)^{0.5}\left(\frac{0.03}{0.673}\right)^{0.1} = 0.11$$

b) $$Bo = \frac{(7.36 \times 10^{-4})(116323)}{(1851)(972.9)} = 4.7541 \times 10^{-5}$$

c) $E = 1 + 24000(4.7541 \times 10^{-5})^{1.16} + 1.37(0.11)^{0.86} = 1.44$

d) $h = 0.023(46714)^{0.8}(1.72)^{0.4}\left(\frac{0.394}{0.0125}\right)(1.44) = 3520$

e) $$S = \frac{1}{1 + (1.15 \times 10^{-6})(1.44)^2(46714)^{1.17}} = 0.591$$

f) $$hpool = \frac{55(0.0046)^{0.12}(116323)^{0.67}}{(-\log(0.0046))^{0.55}(18)^{0.5}}\,0.1761 = 4012$$

g) $h = 3520 + 4012 = 7532$

h) $Q/A = 7532(72.4) = 545316$ Btu/Hr*ft^2

i) $$\text{Deviation\%} = \frac{\text{Predicted Flux - Experimental Flux}}{\text{Experimental Flux}}(100) = 79\%$$